THE ROYAL SOCIETY

The role of Mid-Palaeozoic mesofossils in the detection of early bryophytes

Dianne Edwards

Department of Earth Sciences, Cardiff University, PO Box 914, Cardiff CF10 3YE, UK

Recently discovered Silurian and Devonian coalified mesofossils provide an additional source of data on early embryophytes. Those reviewed in this paper are considered of some relevance to understanding the early history of bryophytes while highlighting the difficulties of recognizing bryophytes in often very fragmentary fossils. The first group comprises sporophytes in which terminal sporangia contain permanent dyads and tetrads. Such spores (cryptospores) are similar to those found dispersed in older Ordovician and Silurian strata, when they are considered evidence for a land vegetation of embryophytes at a bryophyte grade. The phylogenetic significance of plants, where the axes associated with both dyad- and tetrad-containing sporangia are branching, a character state not found in extant bryophytes, is discussed. The second group comprises axial fossils, many with occasional stomata, in which central conducting strands include G-type tracheids and a number of novel types of elongate elements not readily compared with those of any tracheophyte. They include smooth-walled, evenly thickened elongate elements as well as those with numerous branching ± anastomosing projections into the lumen. Some of the latter bear an additional microporate layer, but the homogenized lateral walls between adjacent cells are never perforate. Such cells, which occur in various combinations in central strands, are compared with the leptoids and hydroids of mosses, hydroids of liverworts and presumed water-conducting cells in coeval Lower Devonian plants such as *Aglaophyton*. It is concluded that lack of information on the chemistry of their walls hampers sensible assessment of their functions and the affinities of the plants. Finally, a minute fossil, comprising an elongate sporangium in which a central cylindrical cavity containing spores and possible elaters terminates in a complex poral dehiscence apparatus, is used to exemplify problems of identifying early bryophytes. It is concluded that further progress necessitates the discovery of pre-Upper Silurian fossils with well-preserved anatomy, as well as a re-evaluation of criteria used to assess existing and new Devonian fossils for bryophyte affinity.

Keywords: fossil bryophytes; cryptospores; embryophytes; conducting tissues; phylogeny

1. INTRODUCTION

The inadequacies of the bryophyte fossil record in elucidating their phylogeny and relationships to tracheophytes are legendary. Its critical reappraisal has been stimulated recently by suggestions that distinctive spores recorded from Ordovician rocks, which are considered the earliest evidence of land plants, were produced by plants at the bryophyte grade (Gray 1985; Taylor 1995*a*,*b*, 1997) and by the need to test phylogenetic hypotheses based on cladistic analyses of embryophytes (e.g. Mishler *et al*. 1994). In 1998, Edwards *et al*. reviewed the record, paying particular attention to the characters used in such studies. This paper concentrates on subsequent advances, particularly those involving anatomical and ultrastructural detail derived from small, coalified fossils predominantly of Early Devonian (Lochkovian) age as an example of the potential and frustrations of palaeobotanical contributions. They have been isolated from grey, fluvial, fine-grained sediments excavated from a stream section north of Brown Clee Hill, Shropshire. The mesofossils have already revealed a ground-hugging vegetation made up of plants of diverse affinities in the Late Silurian and Early Devonian (Edwards 1996). They include unequivocal tracheophytes (e.g. *Cooksonia*; Edwards *et al*. 1992) as well as the producers of the spores first recorded in dispersed assemblages in the Ordovician (Wellman *et al*. 1998; Edwards *et al*. 1999). The vast majority of the mesofossils are axial and sterile. Some bear terminal sporangia. Examples of lateral sporangia and axes with enations are very rare. Whether or not the sterile axes are all sporophytic is uncertain. Many show homoiohydric characters typical of 'pteridophyte' sporophytes, but in view of similarities in anatomy (e.g. conducting tissues, stomata) between gametophytes and sporophytes of the Rhynie Chert taxa, *Aglaophyton*, *Nothia* and *Horneophyton*, axial fragments might well derive from gametophytes.

While these fossils are undoubtedly important in documenting past diversity, their value to bryophyte phylogenetic studies, especially relating to origins and inferred pre-tracheophyte early diversification, is somewhat limited by their geological age (figure 1). The Lochkovian examples were formed at a time of major radiations of tracheophytes that occurred some 60 Myr after the first Ordovician spore records—a time interval only 5 Myr shorter than that since the major extinctions at the Cretaceous/Tertiary boundary. This fact should particularly be borne in mind in considering the

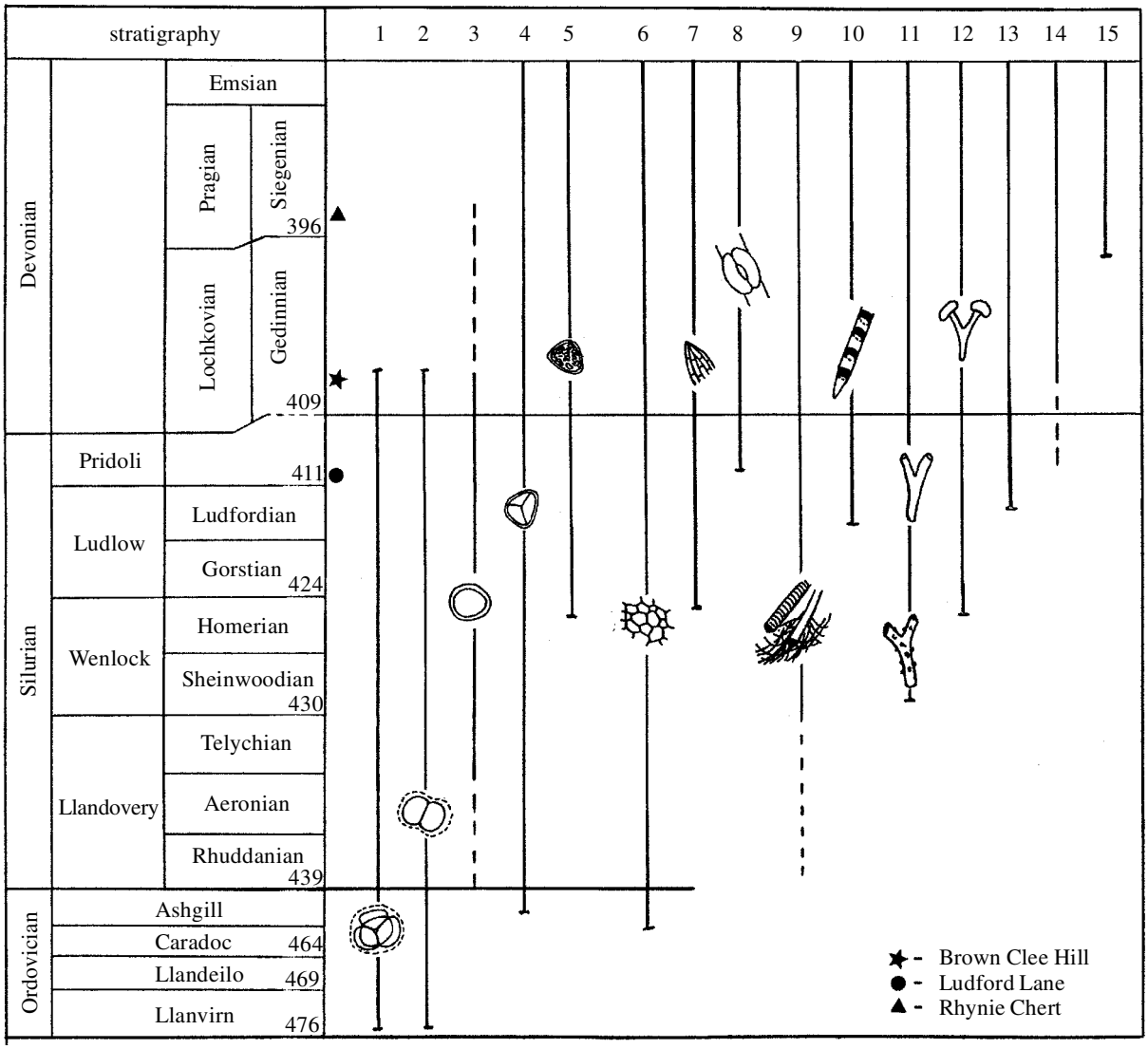

Figure 1. Stratigraphic ranges of fossils mentioned in text. 1, permanent (obligate) tetrads ± envelope; 2, permanent dyads ± envelope; 3, hilate monads; 4, trilete laevigate monads; 5, ornamented trilete monads; 6, cuticular sheets (cf. *Nematothallus*); 7, sporangial cuticles; 8, stomata; 9, associations of tubes, solid line only indicates presence of banded tubes; 10, tracheids; 11, bifurcating axes of ?tracheophyte type; 12, *Cooksonia*/Rhyniopsida; 13, Lycophytina sensu lato; 14, zosterophylls; 15, Trimerophytina.

significance of the dyad- and tetrad-containing fossils reviewed here. The concept that the fossil record shows that the oldest bryophytes were 'contemporaneous with early vascular plants' (Crandall-Stotler 1986; Frey *et al.* 1996) will be explored further in this paper.

2. *IN SITU* CRYPTOSPORES

The earliest evidence for the colonization of the land by higher plants (embryophytes) comes from dispersed microfossil assemblages isolated from Ordovician (Llanvirn) strata (Wellman & Gray, this issue). It is in the form of monads and obligate (also termed permanent) tetrads and dyads (cryptospores sensu Richardson 1988). Megafossils with *in situ* cryptospores, which might be anticipated on gross morphological and potentially anatomical grounds to provide more precise evidence of affinity, are first found in the uppermost Silurian and basal Devonian and will be reviewed in some detail here. The presence of polyads in sporangia raises the possibility that they are immature, and would have split to become trilete or hilate monads before dispersal (see discussion in Edwards *et al.* 1999). This is difficult to refute when such a limited number of specimens is available for comparison except that:

(i) almost all the *in situ* taxa can be referred, at least at generic level, to the dispersed assemblage at the locality;
(ii) with one possible exception (figure 2*j*), transmission electron microscopy (TEM) sections of tetrads do not show the apertural fold that characterizes trilete monads in 'loose' configurations *in situ*;
(iii) neither tetrads nor dyads split into component elements when they are physically and chemically dissociated prior to observation by light microscopy.

In enclosed forms, the persistence of the envelope on dispersal is also conjectural, although even where in TEM sections the layer has a granular and almost discontinuous appearance (e.g. figure 3*g*) it is remarkably resilient

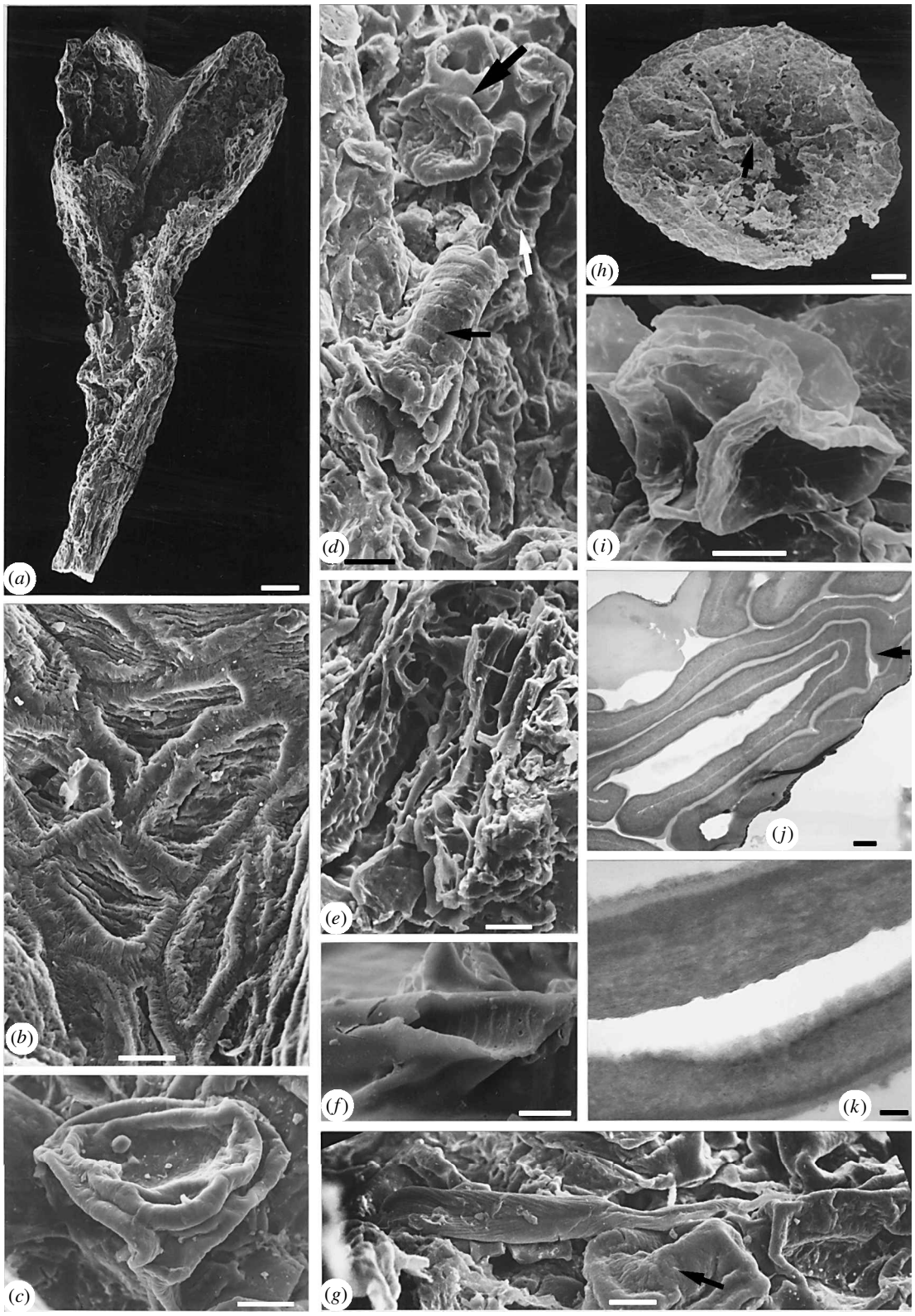

Figure 2. (*a–k*) North Brown Clee Hill specimens, Shropshire. Lochkovian, Lower Devonian. (*a–e,g*) SEMs: *Grisellatheca salopensis*. NMW94.76G.1. (*a*) Entire specimen with bifurcating terminal region. Scale bar = 100 µm. (*b*) Surface at bifurcation. Scale bar = 10 µm. (*c*) *In situ* tetrad with laevigate surface; ?*Cheilotetras*. Scale bar = 10 µm. (*d*) 'Banded' tube in fertile region (small arrows) and remains of spore tetrad (large arrow). Scale bar = 10 µm. (*e*) Longitudinal elements with irregular thickenings from centre of axis. Scale bar = 10 µm. (*g*) Possible elater. Arrow indicates spore tetrad. Scale bar = 10 µm. (*f*) 'Banded' tube attached by amorphous material to surface of a *Tortilicaulis* sporangium. NMW96.5G.9. Scale bar = 10 µm. (*h–k*) ?Cuticle enclosed flattened spore mass. NMW98.23G.3. (*h*) SEM: intact specimen. Arrow indicates possible attachment site. Scale bar = 100 µm. (*i*) SEM: isolated tetrad. Scale bar = 5 µm. (*j,k*) TEMs. (*j*) Part of a tetrad. Arrow indicates possible apertural fold. Note sections through sporangial covering (top left) are of same optical density as outer layer surrounding each spore. Scale bar = 500 nm. (*k*) Trilayered exospore. Lightest layer to outside. Scale bar = 100 nm.

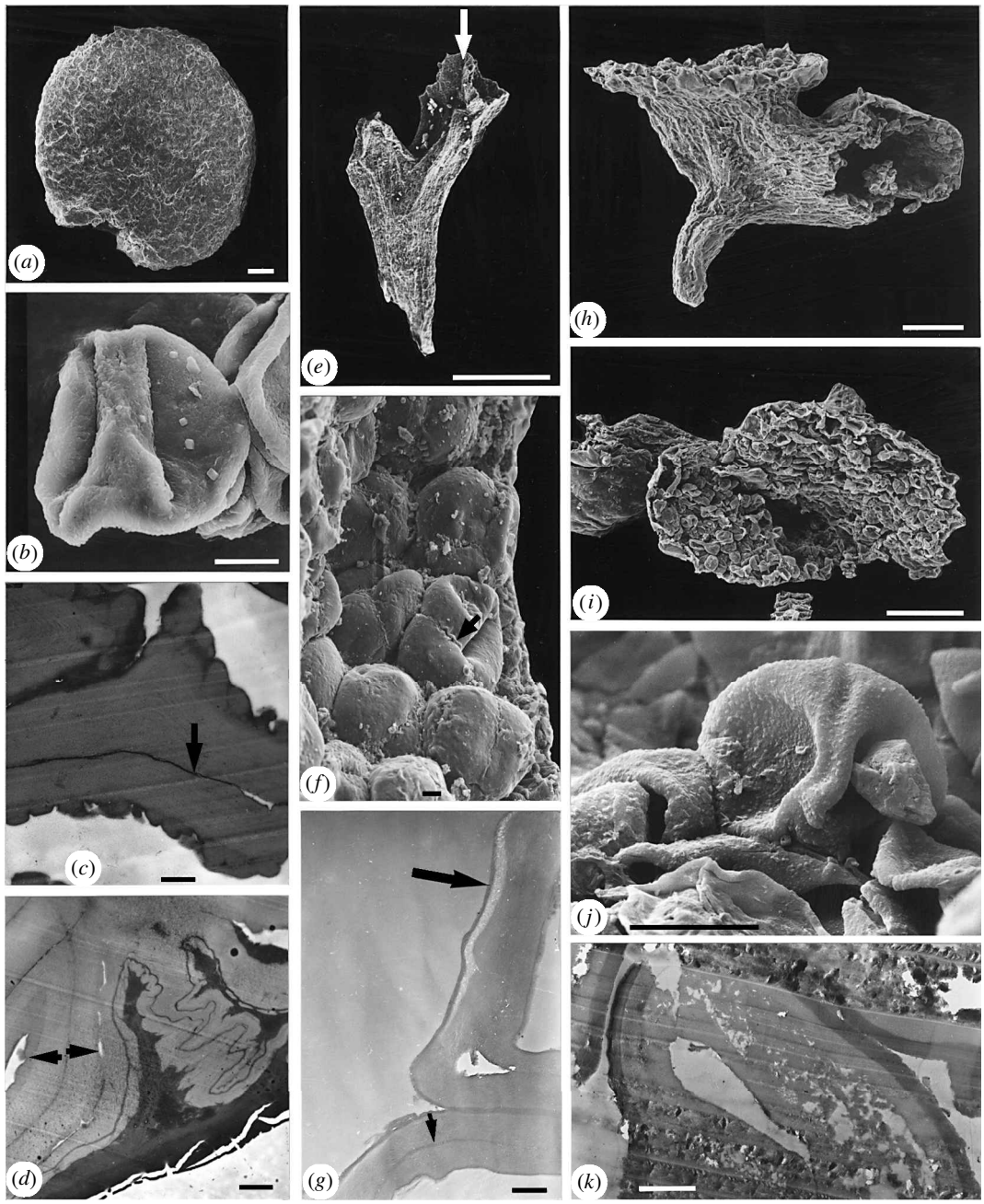

Figure 3. *In situ* permanent tetrads. (*a–d*) Discoidal sporangium with *Velatitetras* sp., Ludford Lane, Shropshire. Pridoli, Upper Silurian. NMW96.11G.4. (*a*) SEM: intact specimen with non-cellular enclosing layer. Possible attachment at bottom left. Scale bar = 100 μm. (*b*) SEM: isolated tetrad with ornamented envelope. Scale bar = 10 μm. (*c*) TEM: exospore ± homogeneous with faint lamellae, and closely adherent envelope. Arrow indicates position of lumen. Scale bar = 500 nm. (*d*) TEM: sporangial covering (dark region) and possible remnants of tapetal material. Arrows indicate limits of single spore. Scale bar = 1 μm. (*e–g*) Axial bifurcating specimen with remnants of terminal sporangium containing *Tetrahedraletes* sp., North Brown Clee Hill, Shropshire. Lochkovian, Lower Devonian. NMW98.23G.2. (*e*) SEM: entire specimen. Arrow indicates base of sporangium. Scale bar = 1 mm. (*f*) SEM: *in situ* naked, laevigate, permanent tetrads. Note typical superficial contact lines (arrow). Scale bar = 10 μm. (*g*) TEM: exospore of two adjacent spores. Note narrow dark layer surrounding each spore, detached in places (large arrow). Small arrow indicates lumen. Scale bar = 500 nm. (*h–k*) Fragment with bases of two terminal sporangia. North Brown Clee Hill locality. NMW96.11G.3. (*h*) SEM: intact specimen. Scale bar = 100 μm. (*i*) SEM: right-hand fertile region (in (*h*)) from above. Scale bar = 100 μm. (*j*) SEM: tetrad with granular envelope. Scale bar = 10 μm. (*k*) TEM: poorly preserved exospore, marginal dark layer represents envelope. Scale bar = 1 μm.

to physical disruption on extraction and subsequent nitric acid treatment, such that it appears as a discrete layer in light microscopy. Another problem relates to recognition of a tightly adhering envelope when only scanning electron microscopy (SEM) studies are possible (e.g. *Grisellatheca*; figure 2*c*).

(a) In situ *tetrads* ± *envelopes*

(i) Grisellatheca salopensis *Edwards* et al. *1999* (*figure 2*a–e, g)

This single specimen, just 1.54 mm long (figure 2*a*), has a bifurcating terminal sporing region with a distinctive, superficial diamond-shaped pattern, the only part of the axial structure in which cells are apparent (figure 2*b*).

The unbranched, non-fertile, axial tissues appear disorganized and are now thought to be highly decayed (p. 19) as evidenced by the 'crater'-like eruptions and 'banded' tubes (figure 2*d*,*f*) (Edwards & Richardson 2000). Some longitudinal 'cells' have irregular transverse outgrowths (figure 2*e*). Hepatic features include the laevigate permanent tetrads and one putative elater (figures 2*c*,*g*). The latter is a strap-shaped structure traversing the sporing region. It bears superficial indentations forming a herringbone pattern. While it is possible that the asymmetric nature of the axis reflects a horizontal ?gametophytic structure with possibly embedded sporangia of riccialean type, it is also possible that it results from incomplete preservation of an erect sporophyte with a terminal bifurcating sporangium. Most axes at the locality, however fragmentary and degraded, are completely surrounded by epidermis or stereome, features not seen in the tetrad-containing plant.

The tetrads themselves have a laevigate surface with complete continuity between adjacent elements, but because they have been examined only by SEM, it is impossible to determine whether or not they possess a closely adhering envelope (and hence belong to *Velatitetras*) or are naked and fused (i.e. without obvious suture and belong to *Cheilotetras*). They are not unlike the tetrads described in the new fertile specimen (p. 19; figure 10*j–n*) although the latter spores show splits between the elements.

Sutures are also visible on the laevigate tetrads in a second bifurcating specimen (figure 3*e*–g; Edwards *et al*. 1999). They are placed in *Tetrahedraletes medinensis*, a taxon also found in the earliest Ordovician assemblages. The spores occur in a cup-shaped depression with an irregular margin, which is assumed to be part of a sporangium terminating a naked axis with irregular, longitudinal, superficial ridges reminiscent of the shrivelled epidermal cells of a rhyniophytoid or tracheophyte. These cells become almost square in the vicinity of the spores, where the sporangial wall itself is many layered. No further anatomical detail was observed.

Two specimens of contrasting morphologies and ages contain unequivocal envelope-enclosed dyads that are assigned to *Velatitetras* (Edwards *et al*. 1999). In both, the envelope is ornamented. The Lochkovian one comprises a naked, forking axis in which each daughter branch ends in a fragmentary sporangium, whose smooth surface with outlines of epidermal cells contrasts markedly with the wrinkled contours of the axis (figure 3*h–k*). Further anatomical detail is not preserved. The second example, unlike the majority of fossils described here, is of late Silurian age and was recovered from marginal marine facies near Ludlow (figure 3*a–d*). It comprises a disc-shaped spore mass encased in a non-cellular homogeneous layer. SEMs show deep invagination of the envelope between constituent spores and, where it has disintegrated in this region, laevigate spores beneath. TEMs of the two kinds of *Velatitetras* suggest that they are not closely related. Although in both the exospore is single-layered, in the Silurian spores there are traces of lamellation following the spore contours (figure 3*c*) but the younger ones have a granular exospore (figure 3*k*). In the latter, the envelope is more electron-dense and tightly adhering, its ornament low and irregular. The ornament of the Silurian envelope is far more pronounced, its indentations extending almost to the surface of the exospore. Again it is closely adherent. Towards the outside of the spore mass, the envelope is continuous with the innermost layers of the sporangial wall, suggestive of involvement of a tapetal layer (figure 3*d*).

In the final example (figure 2*h–k*; Edwards *et al*. 1999), cryptospore relationships are less clear-cut. The specimen is a discoidal spore mass surrounded by a layer of cuticle, in which puckering to the centre of one surface suggests attachment to an axis (figure 2*h*). The spores are in tetrads with pronounced invaginations between the units (figure 2*i*). Distal surfaces are invaginated. They are laevigate or bear fairly evenly spaced but irregularly shaped outgrowths. Spore walls are tri-layered with each layer (distinguished by differing electron opacity) completely surrounding individual spores (figure 2*j*,*k*). There is a distinct thickening, particularly of the middle layer, in the vicinity of the equator and a possible apertural fold at the 'junctions' of proximal poles (figure 2*j*). The latter is a characteristic of trilete spores. This feature and the more ready separation of the tetrad individuals when prepared for TEM and light microscopy (LM) mitigate against affinity with cryptospores. However, triradiate marks were not apparent in LM. Similar exospore ultrastructure is not seen elsewhere. Three layers reported on the distal exposed surfaces of the Late Ordovician/Early Silurian dyad *Dyadospora murusattenuata* (type 1) include a middle, lamellated layer (two to three lamellae) and an inner spiny one, and thus are not comparable with the ultrastructure in the tetrads here, where tri-layering extends around each spore (Taylor 1997).

Diversity in ultrastructure also characterizes masses of smooth-walled, naked tetrads recovered from the matrix. Particularly complex are naked tetrads similar to *Tetrahedraletes*, in which individual monads show some separation. The outer third of the exospore is homogeneous, the remainder is made up of granules or lamellae (Edwards *et al*. 1999, figs 105, 106, 113).

(b) In situ *dyads*

In one case only, an unbranched axis, 1.2 mm long, is terminated by a well-defined, beaker-shaped sporangium with intact truncated apex (figures 4*d*,*e*). *Cullulitheca richardsonii* has naked laevigate dyads with a pronounced suture and invaginated distal surfaces (figures 4*f*,*g*; Wellman *et al*. 1998) enclosed in a sporangium wall showing no cellular detail. The axis itself has a superficial, shrivelled appearance and also lacks any indication of cells. The exospore is homogeneous, with no evidence of any envelope (figure 4*h*). Such spores were assigned to *Dyadospora murusdensa* Strother & Traverse emend Burgess & Richardson (1991), although the latter only rarely have distally invaginated surfaces. In contrast a second dyad-containing specimen, *Fusitheca fanningiae* (figure 4*i*,*j*; Wellman *et al*. 1998) has a fusiform terminal sporangium at the tip of one branch of an isotomously branching naked system (figure 4*i*), and the dyads themselves, although distally invaginated, have a closely adherent, thin envelope (figure 4*j*). TEM studies reveal a homogeneous exospore. Individual cells could not be seen on the wrinkled surface of the axis, although the fractured end showed a reticulum of homogenized walls surrounding

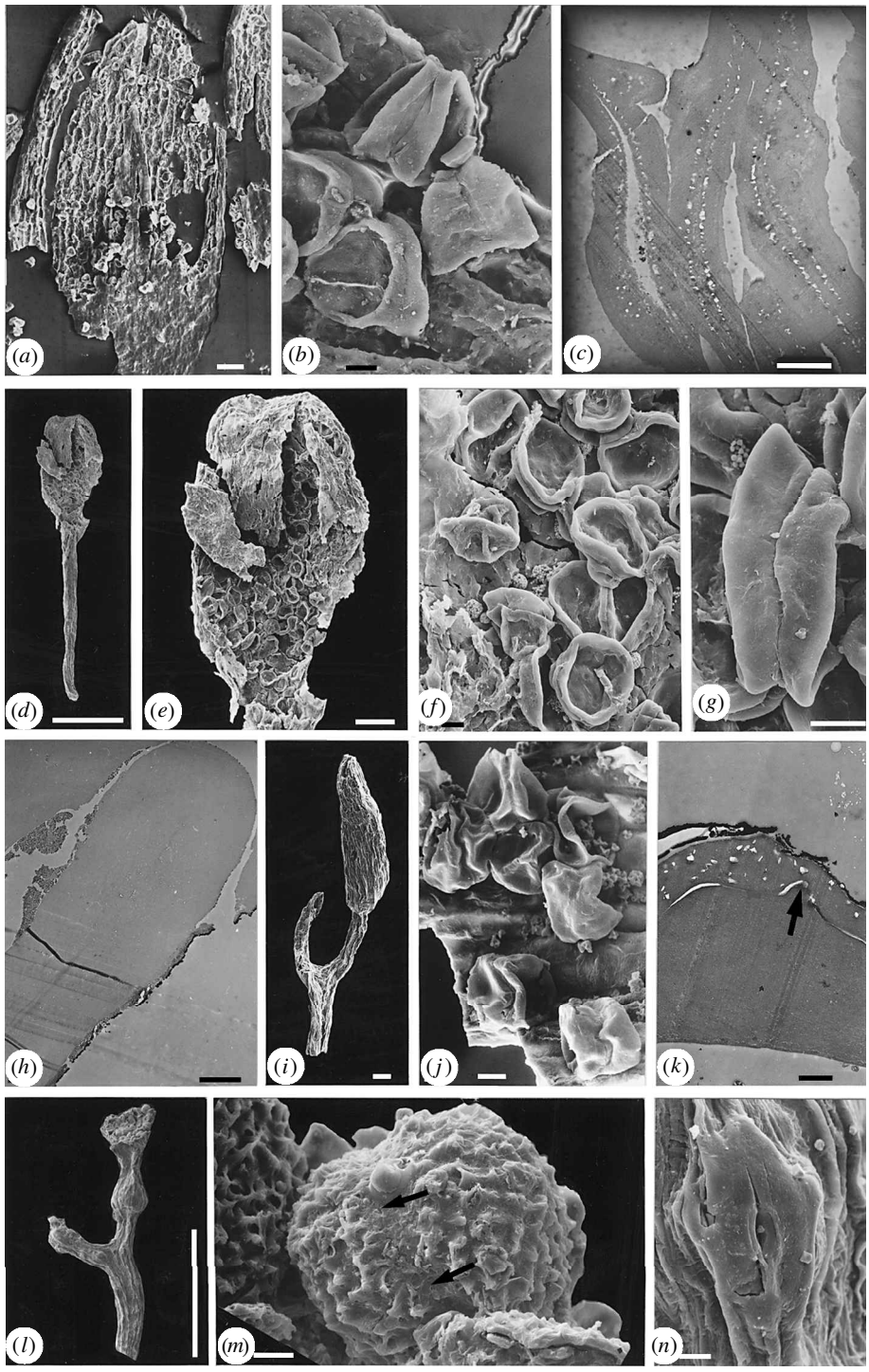

Figure 4. *In situ* permanent dyads. All North Brown Clee Hill, Shropshire. Lochkovian, Lower Devonian. (*a–c*) Sporangial cuticle with adhering laevigate dyads. NMW97.42G.1. (*a*) SEM: central cuticle probably representing one complete valve. Scale bar = 100 µm. (*b*) SEM: cluster of probably naked dyads with deeply invaginated distal surfaces. Scale bar = 10 µm. (*c*) TEM: walls of several spores. Note row of voids close to lumen in otherwise homogeneous exospore. Scale bar = 250 nm. (*d–h*) *Cullulitheca richardsonii*. NMW96.11G.6. (*d*) SEM: entire specimen. Scale bar = 500 µm. (*e*) SEM: sporangium enlarged. Scale bar = 100 µm. (*f*) SEM: *in situ* laevigate dyads with distal invaginations. Scale bar = 10 µm. (*g*) SEM: single dyad showing contact feature. Scale bar = 10 µm. (*h*) TEM: homogeneous exospore with some attached extra-exosporal material. Scale bar = 1 µm. (*i, j*) SEMs: *Fusitheca fanningiae*. NMW97.42G.4. (*i*) Intact specimen. Scale bar = 100 µm. (*j*) Laevigate dyads attached to inside of sporangial wall. Scale bar = 10 µm. (*k–n*) Naked bifurcating axis with vestiges of a terminal sporangium. NMW99.19G.1 (courtesy of K. Habgood). (*k*) TEM: homogeneous exospore and envelope with voids. Arrow indicates ornament on spore. Dark line is gold coating. Scale bar = 500 nm. (*l*) SEM: intact specimen. Swelling on axis is probably a taphonomic artefact. Scale bar = 1 mm. (*m*) SEM: single tetrad with envelope. Arrows indicate position of contact between spores. Scale bar = 10 µm. (*n*) SEM: stoma. Scale bar = 10 µm.

irregularly shaped lumina and a central irregular homogenized area. The sporangial wall appears to be single-layered, comprising tubular to spindle-shaped cells with uniformly thickened lateral walls and some irregular bars crossing the lumen. The walls lining the sporangial cavity are minutely reticulate.

A further bifurcating specimen currently being investigated by Kate Habgood (Cardiff University) is unique in that the envelope-enclosed dyads are ornamented and the axes bear stomata (figure 4*k–n*). Evidence for the two guard cells is indirect; the stomatal pores are extended into short slits in the position of the common walls and there are polar indentations (figure 4*n*). TEM sections show that the exospore is homogeneous with superficial coni, and that these are draped by a uniformly thick layer containing voids (figure 4*k*). In some examples, this layer covers the junction between the spores, and is hence interpreted as an envelope. There is no similarly enveloped, ornamented, permanent dyad taxon in the dispersed spore record. Hilate cryptospores with similar exospore ornament at the locality would be placed in *Chelinohilates horridus* (Richardson 1996), but there are no indications whatever of splitting in the *in situ* examples.

The North Brown Clee locality has yielded some sporangial cuticles with adhering permanent dyads. Most notable is an ovate example with a discrete outline (?representing a valve) and linear rectangular 'cells', which bears extremely thin-walled dyads with sporadic preservation of an envelope (figure 4*a*,*b*; Wellman *et al*. 1998). The latter is homogeneous and differentially stains in TEM sections (figure 4*c*). The exospore itself is also homogeneous except for a zone of voids close to the lumen. Homogeneous exospores also characterize groups of laevigate, permanent dyads with some variation in wall thickness and degree of invagination of the distal surface (Wellman *et al*. 1998). Such ultrastructural uniformity is disappointing as spore masses or isolated sporangia with hilate dyads, i.e. separated cryptospores with large circular contact area lacking a trilete mark, show far greater variation. All are laevigate and would be assigned to *Laevolancis divellomedia* sensu lato—a taxon currently being further subdivided by J. B. Richardson. Wellman *et al*. (1998) distinguished five broad-exospore ultrastructural types. The only one with an entirely homogeneous exospore was recovered from a small, discoidal sporangium. The remainder are bilayered in both proximal and distal walls thus contrasting with the *in situ* forms described above where the contact faces show only one layer. They also show traces of lamellation, one even with white-line-centred lamellae. Preservation of such delicate structures demonstrates that the homogeneity of the walls in the *in situ* permanent dyads and tetrads from the same locality is not caused by diagenesis. However, such ultrastructural simplicity, mirrored in early dispersed taxa such as the Late Ordovician/Early Silurian *Tetrahedraletes medinensis* (Taylor 1995*a*) and *Pseudodyadospora* sp. (Taylor 1996) frustrates attempts to detect affinities using this character.

(c) *General discussion on mesofossils with* in-situ *cryptospores*

The mesofossils described here are united in that they contain polyads, resembling, at least superficially, the permanent or obligate cryptospores recorded from coeval strata and from rocks extending *ca*. 60 Myr back into the Ordovician. Where subtending structures are preserved, they are naked axes and the sporangia are terminal. Representatives of both dyad- and tetrad-containing plants show isotomous branching. Axes are very short in unbranched representatives and so it is impossible to conclude that branching was absent. In one case only, viz *Grisellatheca* (figure 2*a–e*,*g*), it was speculated that the axial fragment is a gametophyte, with deeply seated sporangia, but this was dismissed as the tissues surrounding the spores are superficially quite distinct from the rest of the specimen. The fossils are therefore all interpreted as sporophytes and derived from plants of small stature. They probably should all be placed in different genera.

(i) *Comparisons with dispersed spores*

In contrast to information on *in situ* spores, the majority of dispersed spores, particularly from older strata, have been described and named from LM studies. Combined LM and TEM studies such as those recently undertaken on dispersed spores from the North Brown Clee Hill locality are essential for accurate identification (Richardson 1996). This is especially so for distinguishing between fused (sensu Wellman & Richardson 1993) polyads and forms with closely adhering envelopes, and for deciding whether or not fused or unfused when an envelope is present. The distally inflated, envelope-enclosed dyads from *Fusitheca fanningiae* provided a good illustration for the latter. If fused, the dyads would be placed in *Segestrespora laevigata*; if unfused, in *Abditidyadus laevigatus*. These spores also superficially resemble the naked *Pseudodyadospora* whose identification depends on the nature of the contact areas (hidden in SEM). Ultrastructural studies eliminate identity, at least, with Ashgill/Llandovery *S. membranifera*. *Abditidyadus laevigatus* ultrastructure is unknown, but similarly dated *Pseudodyadospora* sp. is homogeneous.

Two specimens contain *in situ* tetrads that are unequivocally membrane-bound and hence would be placed in the dispersed taxon *Velatitetras*, a genus that encompasses both smooth and ornamented envelopes and has been recorded from the Lower Devonian. Neither shows ornament identical to published spores. The Silurian form (figure 3*a–d*) in the discoidal sporangium is closest to *V. anatoliensis* Steemans, le Herisse & Bozdogan 1996, whose range extends from Ordovician to Early Silurian. The Lower Devonian examples in sporangia terminating a bifurcating axis (figure 3*h–k*) have no close counterparts in dispersed species. The ultrastructure both of exospore and envelope of the two *in situ* forms is quite different, with only the Silurian form showing traces of exospore lamellae, but there are no published reports of similar ultrastructure in dispersed spores. The remaining examples are laevigate. Those of *Grisellatheca* (figure 2*c*) demonstrate the problems of describing spores solely from SEM studies. If naked, fused tetrads, they would be assigned to *Cheilotetras*; if with closely adherent envelope to *Velatitetras*. Laevigate, unfused forms (i.e. with sutures separating spores) assigned to *Tetrahedraletes* occur in the bifurcating specimen (figure 3*e–g*), and in a number of spore masses. While ultrastructural studies have been

useful in demonstrating diversity in these laevigate forms, the most complex exospores, comparable with the lamellate exospores of *Dyadospora murusdensa* (Taylor 1995*a*, 1996) and *D. murusattenuata* in part (Taylor 1997), are in spore masses. The only illustrated ultrastructure from Upper Ordovician tetrads is from *Tetrahedraletes medinensis* where the exospore is homogeneous (Taylor 1995*b*) and thus similar to some of the Lower Devonian examples (see Edwards *et al*. 1999; figure 3*g*) although an exfoliating outer layer has not been reported in the older forms.

Such comparisons show that while configurations of the mature spores indicate that the reproductive biology of the producers remained unchanged from Ordovician to Lower Devonian times, we have no compelling evidence as yet that the *in situ* spores are conspecific with earlier dispersed examples. More evidence is required on the ultrastructure of cryptospores in dispersed assemblages through time, especially as limited data from trilete spores suggest that spore ultrastructure has some taxonomic value, and can show stasis when spore ornament changes (e.g. Fanning *et al*. 1988).

(ii) *Affinities of the mesofossils*

Spore ultrastructure

The spores in the mesofossils show none of the lamellate ultrastructure that was used to invoke hepatic, more precisely sphaerocarpalean, affinity in dispersed dyads from the Ashgill/Ordovician (Taylor 1995*b*, 1997). The essentially homogeneous exospore in the majority is characteristic of anthocerotes and bryopsid mosses, although the latter sometimes have a very narrow and inconspicuous layer that is basal or within the homogeneous part (Brown & Lemmon 1990). If indeed the envelope is homologous with perispore (Gray 1991; Edwards *et al*. 1999), this is a further similarity with mosses, although perispore also occurs in homosporous ferns, where, in general, a thick, outer homogeneous layer overlies a lamellate one (Lugardon 1990). However, in many spores, both bryophytic and 'pteridophytic', sporopollenin deposition has obliterated the lamellation present in all developing spores, producing homogenization at maturity. Thus in these Lower Devonian spores, ultrastructure is not useful in determining broad phylogenetic affinities, although minor variations in exospore and envelope may be useful in revealing relationships between coeval plants.

Spore configuration

It was the tetrad organization of dispersed Ordovician and Silurian spores that led to the hypothesis of their bryophyte affinity (Gray & Boucot 1971; Gray 1985, 1991) based on the retention of this feature in hepatics, e.g. *Sphaerocarpos*, *Riccia*, *Cryptothallus* and certain mosses. Extant analogues for dyads are far less common but occur in bryophytes (e.g. Schuster 1967; Bell 1992), *Selaginella* (Graustein 1930) and ferns (Morzenti 1967; Hickok & Klekowski 1973). In the majority of cases, they result from abnormal meiosis, frequently associated with hybridization, and occur together with trilete spores in the same sporangia. Our studies show conclusively that all spores in sporangia are dyads and are not the products of meiotic failure. The producers display a type of reproductive biology no longer found today.

Gross morphology

Isotomously branching axes with terminal sporangia characterize early tracheophytes, e.g. *Cooksonia* (Edwards *et al*. 1992), and a complex of plants producing trilete spores, e.g. *Salopella*, *Tortilicaulis* (Edwards *et al*. 1994) and *Pertonella* (Fanning *et al*. 1991), in which xylem anatomy has not been demonstrated and which are therefore termed rhyniophytoid.

Absence of axial anatomy in the cryptospore-producing plants is a major frustration, which will be eased only by the discovery and analysis of further specimens. The finding of stomata on one dyad-containing plant with branching axes and the sterile axes with anomalous conducting tissues (p. 7) demonstrates some progress. While clearly premature to place too much emphasis on such preliminary findings, the occasion of a symposium such as this provides a forum to raise some very tentative hypotheses (admittedly involving too many generalizations) that will be supported or disproved only by the discovery of further fossils in Ordovician and Silurian rocks.

Thus considering the affinities of the mesofossils, the following are, inter alia, possible.

(i) The plants comprised relict populations of those that existed in Ordovician times, and hence based on the presumed affinities of the *in situ* cryptospores, are bryophytes with branching sporophytes. Such a hypothesis finds no support in cladistic analyses (e.g. Mishler & Churchill 1984). However, in *Grisellatheca*, in particular, admittedly very poorly preserved axial anatomy finds no similarities with that in later tracheophytes. Those with stomata suggest greater affinity with mosses than liverworts, raising the possibility that branching evolved early in moss evolution and was subsequently lost. Anatomical evidence is required to support this.

(ii) The spores are plesiomorphic and the plants are stem-group tracheophytes in which branching in sporophytes preceded the separation of spores. Such plants could comprise relict populations of those that existed prior to monad evolution in the latest Ordovician or those subsequent to acquisition of stomata. Support for this hypothesis requires demonstration of tracheids in the subtending axes, with or without stomata.

3. CONDUCTING TISSUES IN MESOFOSSILS

The demonstration that each of the three major clades of early vascular plants is characterized by a particular tracheidal architecture augurs well for the use of anatomical features of water-conducting cells in the assignment of leafless axial forms at least to a higher taxon (Kenrick & Crane 1991; Kenrick *et al*. 1991*a*,*b*). There is also, but far more limited evidence, suggesting that certain species of *Cooksonia* possessed far simpler conducting cells (viz thick-walled tubes with additional internal annular thickenings; Lang 1937; Edwards *et al*. 1992), while the Rhynie Chert, *Aglaophyton major*, displays yet another kind, which has been compared with moss hydroids (Edwards, D. S. 1986). Such tracheary diversity in early vascular plants, coupled with information on extant bryophyte conducting

tissues (e.g. Hébant 1977, 1979) prompted a detailed anatomical analysis of sterile, coalified axes, both branched and unbranched from Upper Silurian and Lower Devonian strata, the preliminary results of which are presented here. The mesofossil fragments are normally less than 3 mm long, and a fraction of a millimetre in diameter. They rarely show branching. Where superficial features are well-preserved, outlines of epidermal cells and an occasional stoma are visible. Two guard cells are rarely well-defined, but their presence is inferred from polar indentations. Stomatal density is thus always very low (cf. Edwards 1998). A two- to three-layered stereome may be present, and in a few examples, cell walls are preserved (if imperfectly) throughout the axes. Some axes show a discrete central strand that readily separates from the remaining, usually more poorly preserved, tissues. In others, only a variation in anatomy, often acccompanied by better preservation, marks the position of central conducting tissues. In a very few examples, the entire fossil comprises tracheids, always of G-type.

(a) *G-type tracheids*

G-type tracheids (named after the Lower Devonian *Gosslingia*: Kenrick *et al.* 1991*a*) characterize the zosterophyll–lycophyte clade. They were distinguished because the presumed primary wall between conventional annular and spiral secondary thickenings is covered by an additional perforated and assumed lignified layer. Configurations of coalified material and pyrite in permineralizations of *Gosslingia* were explained in terms of the relative decay of cellulose and lignin combined with the bacterial production of pyrite (Kenrick & Edwards 1988). Detailed ultrastructure was deduced by a process involving acid etching, and it revealed that pyrite was precipitated in cell lumens and in spaces occupied by relatively biodegradable polymers such as cellulose. Thus any coalified material remaining in the fossil (viz secondary thickenings and intervening layer) was interpreted as once lignified. Figure 5*a* shows a strand of transversely fractured typical G-type tracheids; extra-xylary tissues are largely missing or have been 'condensed' into a homogenized rind. In this specimen, pyrite occurs only in the tracheary lumina such that the coalified walls comprise both cellulose and lignin residues, and are interpreted as a more faithful replica of original architecture. Comparisons between the two forms of preservation will thus permit assessment of the extent to which ultrastructure may have been affected by permineralization. As analysis of the latter involves destructive acid-etching techniques, these coalified specimens allow, for the first time, detailed description of individual elements and their spatial relationships. Here I concentrate on the specimen illustrated in figures 5 and 6*a–c*. As is characteristic of the clade as a whole, the xylem is not centrarch, but shows a wide range of diameters, even in the central part, presumably reflecting the tapering of tracheids (figure 5*a*). There is no well-defined zone of 'protoxylem' (insofar as it can be identified in fossils). Its presence is inferred from a very narrow, crushed, peripheral layer in which jumbled fragmentary secondary thickenings are apparent.

Conventional secondary thickenings range between simple (figure 5*c*,*g*), directly attached annular (figure 6*c*; sensu Bierhorst 1960), to spiral (figure 5*b*) to reticulate (figure 5*f*). The latter are rare and found towards the centre. In one tracheid only, globules, singly or in small clusters, are continuous with a secondary thickening (figure 5*e*). The vast majority are coalified throughout. A few show a small void (triangular in cross section) at the junction with the lateral wall (figure 5*g*).

The secondary thickenings show variation in diameter and distance apart between tracheids but individual tracheids have a uniform appearance. The persistent wall between the secondary thickenings (indeed the latter appear as an integrated part of this wall) is perforated by circular to irregular holes whose size and frequency vary between tracheids. Uncommon are examples where holes are small (< 100 nm) and widely spaced. Larger examples (*ca.* 1.2 μm) tend to be more irregular in outline and may occupy most of the wall such that it tends to break down. Fractured transverse sections (figure 5*b–d*) and superposed cells (figure 6*a*) show that holes in adjacent cells may or may not be coincident and are always of different size. Thus in some cases there is continuity between lumina of adjacent tracheids (arrows in figure 5*b*,*c*). However, it is doubted that this was the case in the functioning plant (see also in *Gosslingia*; Kenrick & Edwards 1988). Studies of decay of xylem (mainly conifer, e.g. Dunleavy & McQuire 1970; Levy 1975) have shown that pit-closing membranes (primary cell wall and middle lamella) are rapidly attacked and removed by bacteria soon after the death of the plant, thus increasing permeability of the tissue for further infection. It seems not unlikely that this process occurred during waterlogging of the plant fragment prior to burial and fossilization. Indeed the presence of such membranes in transpiring plants would have been essential to reduce cavitation.

Considering the relationship between the perforated layer and the thickenings, the schematic reconstruction of the *Gosslingia* tracheid (Kenrick & Edwards 1988, fig. 26*c*) shows the secondary thickenings as inwardly directed, non-perforate extensions of the perforate layer, with a core continuous with a layer of presumed cellulose, approximately twice as wide as the perforate layer. Such a detached outer layer is not apparent in these coalified examples where the perforations extend to the junction between adjacent cells. If correct in assuming the original presence of a pit-closing membrane, this suggests that the original primary cell wall of the tracheid was very thin, and homogenized with the wall between perforations in the intervening layer. In rare specimens where adjacent tracheids have separated in this area, there is some evidence of grooves in the secondary thickenings (figure 5*g*), possibly demonstrating an originally thicker cellulose wall in these examples as in *Gosslingia*. In the majority of cases, however, when viewed from the outside of the cell, the perforate layer is more or less continuous in the vicinity of the tracheids (e.g. figure 6*a*,*b*). Such observations raise the possibility that the wide zone between the perforated layers in *Gosslingia* is at least partially an artefact of pyrite permineralization: a hypothesis that is currently under experimental investigation at Cardiff. That the total wall thickness in these Lochkovian tracheids is narrower than the coalified layer plus pyrite in *Gosslingia* may be of some relevance, but diminished in that the same taxon is probably not

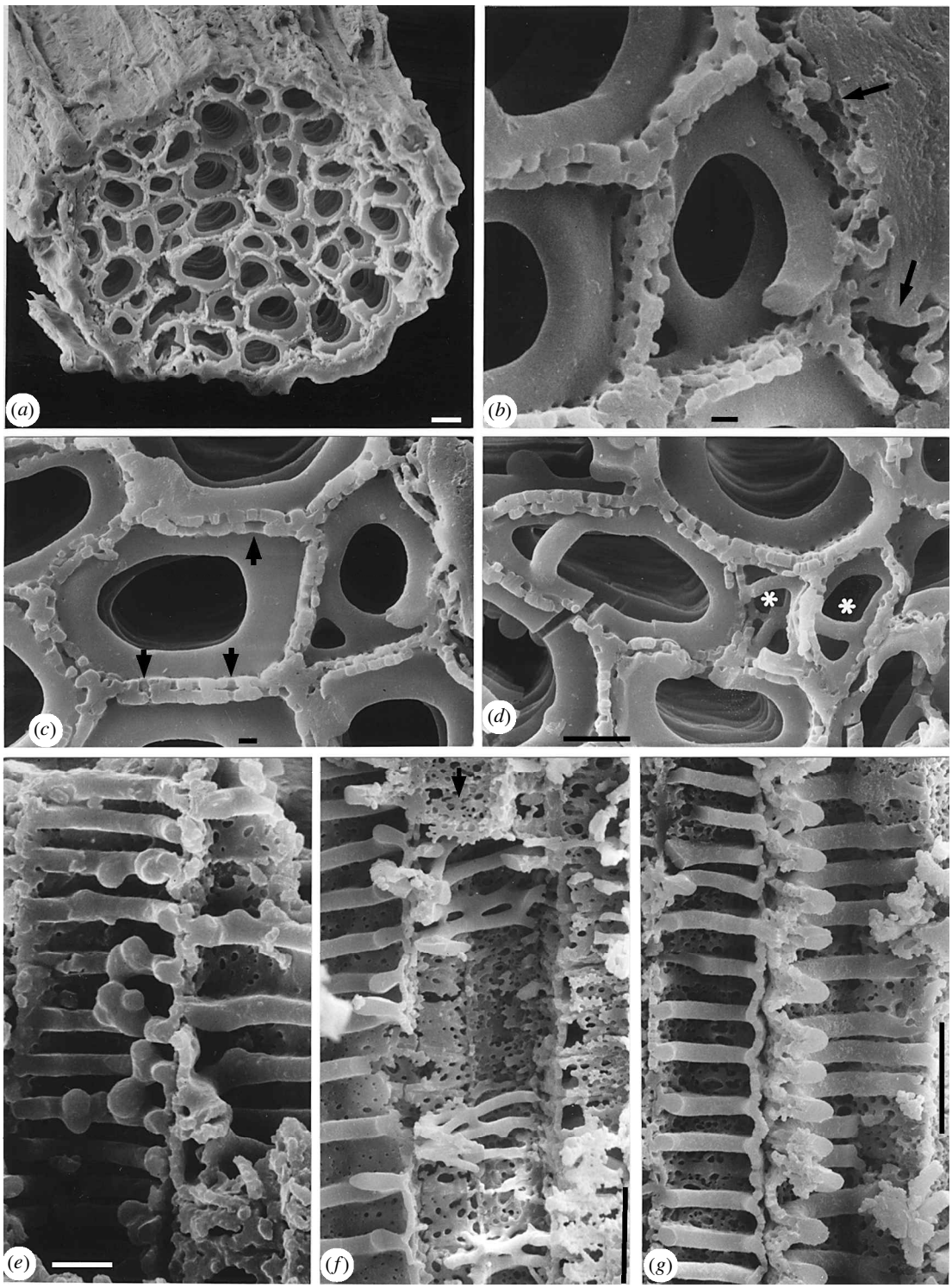

Figure 5. SEMs: coalified strand with G-type tracheids. North Brown Clee Hill, Shropshire. Lochkovian, Lower Devonian. NMW99.20G.1. (*a*) Fractured cross-section TS. Note homogeneous 'rind' of peripheral tissues. Scale bar = 10 μm. (*b*) Fractured TS of spiral tracheid. Arrows indicate position of crushed presumed protoxylem. Scale bar = 1 μm. (*c*) Fractured TS. Note intact annular thickening, and juxtapositioning of the pitting in the interconnecting walls of adjacent tracheids. Arrows indicate apparent perforations. Scale bar = 1 μm. (*d*) Fractured TS. Tracheid complex at centre of strand. Asterisks indicate possible terminations of tracheids. Scale bar = 5 μm. (*e*) Fractured longitudinal section (LS) showing unusual globular projections on annular secondary thickenings. Scale bar = 5 μm. (*f*) Fractured LS with reticulate pitting. Arrow indicates intervening wall viewed from outside (i.e. by separation of the middle lamella). Scale bar = 10 μm. (*g*) Fractured LS of two adjacent tracheids with separation at the middle lamella. Note inter-tracheid variation in dimensions and spacing of annular thickenings, which are homogeneous in cross-section. Scale bar = 10 μm.

involved. In contrast, Cook & Friedman (1998) have postulated that the areas of pyrite within cores of secondary thickening and outside the recalcitrant intervening wall in permineralized G-type thickenings occupy mainly the same regions as the degradation-prone, template layer described in *Huperzia* tracheids, while lignified resistant layers correspond to the coalified secondary thickenings and intervening layers. Their

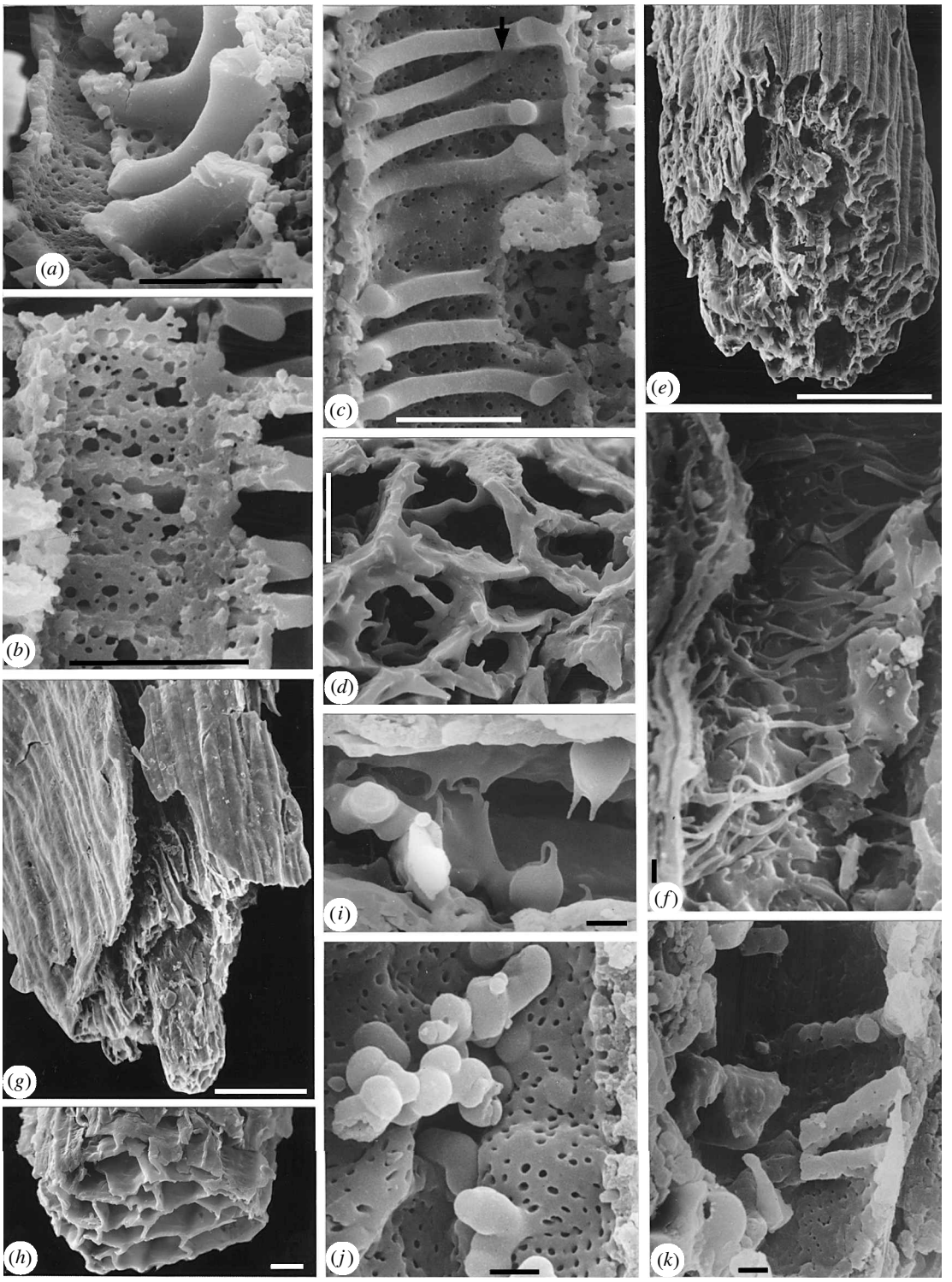

Figure 6. SEMs of presumed conducting tissues. North Brown Clee Hill, Shropshire. Lochkovian, Lower Devonian. (*a–c*) NMW99.20G.1. (*a*) Fractured tracheids demonstrating difference in dimensions of pitting in intervening layers of adjacent cells. Scale bar = 10 µm. (*b*) Outside of the tracheid wall as viewed from the middle lamella. Note lack of any major discontinuity associated with positions of the secondary thickenings. Scale bar = 10 µm. (*c*) Longitudinal fracture where secondary thickenings are less regular and probably interconnected (arrow), and small pits in intervening layer. Scale bar = 10 µm. (*d*) Axial fragment with central strand. Transversely fractured strand. Surfaces of internal walls of individual cells are smooth and extend into lumen, sometimes forming an irregular net. NMW99.20G.2. Scale bar = 10 µm. (*e,f*) Smooth axis. NMW99.20G.3. (*e*) Transverse fracture with intact epidermis of cells with evenly thickened walls. Arrow indicates cell magnified in (*f*). Scale bar = 100 µm. (*f*) Longitudinal fracture of cell with dendritically branched, smooth, wall projections. Scale bar = 1 µm. (*g,h*) Axis with discrete central strand. NMW99.20G.4. (*g*) Irregular fracture showing smooth surface with faint indications of epidermal cells. Scale bar = 100 µm. (*h*) Fractured TS of strand composed of cells with walls of uniform thickness. Scale bar = 10 µm. (*i–k*) Longitudinally fractured central cells from smooth axis. NMW99.20G.5. Scale bars = 1 µm. (*i*) Cell with smooth internal surfaces and globule- to strand-like projections. (*j*) Cell with microperforate layer lining lumen with globular projections. (*k*) Cell with microperforate layer extended into horizontal rod-shaped structures.

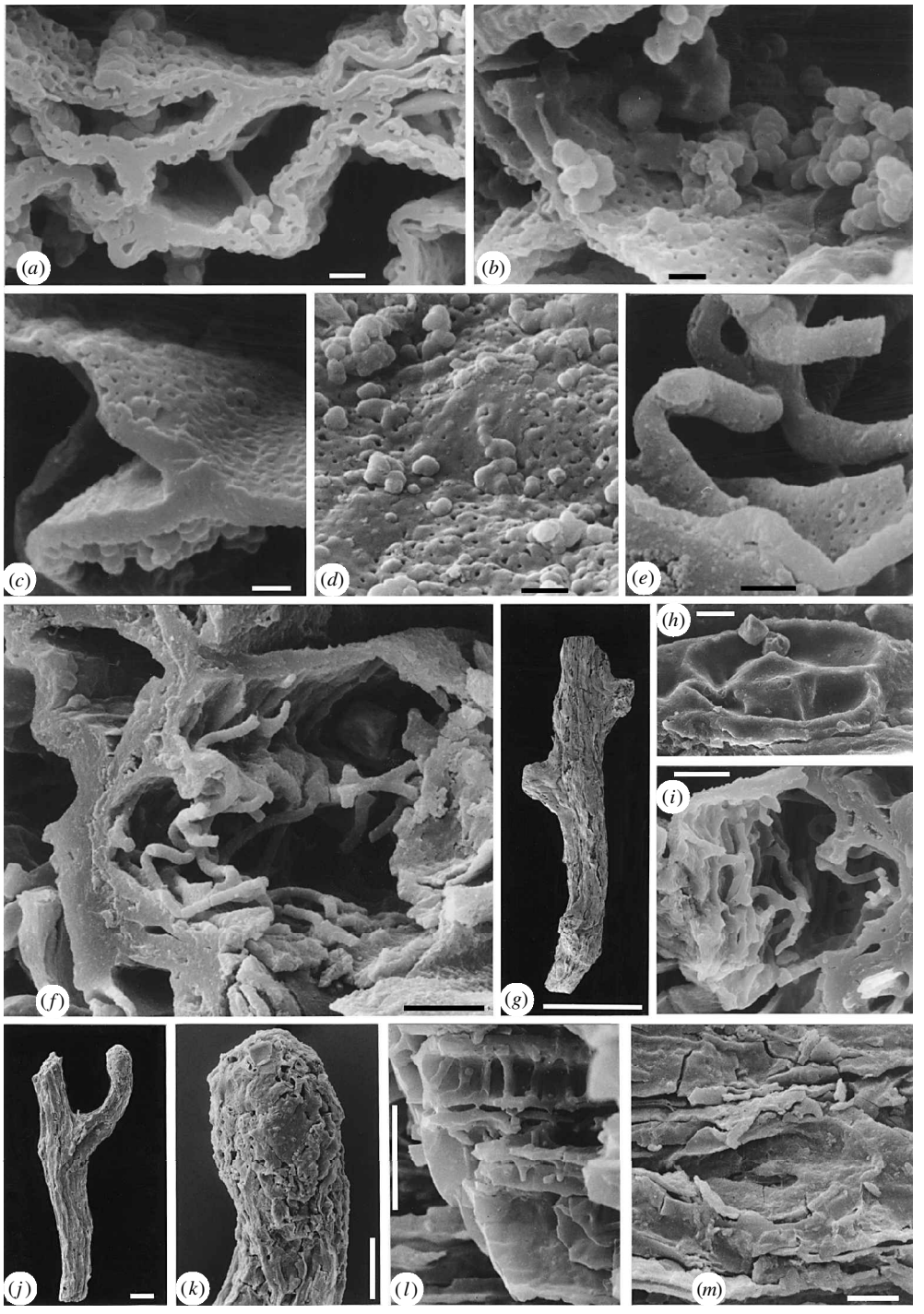

Figure 7. SEMs of presumed conducting tissues. North Brown Clee Hill, Shropshire. Lochkovian, Lower Devonian. (*a–d*) Central cells of transversely fractured axis. NMW99.20G.6. Scale bars = 1 μm. (*a*) Group of cells with homogenization of common walls and layer lining the lumen with pores. (*b*) Lumen partially occluded with numerous fused globules. (*c*) Junction of three cells, in which microperforate lining layer is not well developed. (*d*) Superficial appearance of microperforate layer with adhering globules. (*e*,*f*) Central cell from axis with complex thickenings extending into lumen. NMW99.8G.20. (*e*) Detail from (*f*) showing microperforate layer covering the projection. Scale bar = 1 μm. (*f*) Transversely fractured cell with complex 'tortuous' projections. Scale bar = 5 μm. (*g–i*) Axis with enations. NMW99.20G.7. (*g*) Intact specimen. Scale bar = 1 mm. (*h*) Stoma. Scale bar = 10 μm. (*i*) Central cell with complex projections in transversely fractured axis. Scale bar = 5 μm. (*j–m*) Branching axis with one complete tip. NMW99.20G.8. (*j*) Intact specimen. Scale bar = 100 μm. (*k*) Slightly swollen intact tip. Scale bar = 50 μm. (*l*) Longitudinally fractured central cells, with simple annular thickening (longitudinal axis across figure). Scale bar = 10 μm. (*m*) Stoma on poorly preserved surface. Scale bar = 10 μm.

schematic of a G-type tracheid also shows a primary cell wall. Unfortunately, complete homogenization of the wall in the coalified fossils precludes testing of their hypothesis.

(b) Cooksonia-*type tracheids* (*figure* 7j–m)

Figure 7 shows a bifurcating axial fragment in which a narrower daughter branch terminates as a slight swelling (figure 7*k*). The latter lacks the superficial longitudinal

wrinkling seen on the rest of the specimen, where rare stomata are present (figure 7*m*), and longitudinally orientated cell walls were not apparent on breaking it open. Spores could not be identified, but it is tempting to conclude that this swollen tip was an immature sporangium. The fractured proximal end shows cellular organization except for a couple of elongate longitudinally orientated elements with transverse, annular thickenings. The cells are narrow (< 5 μm diameter), and show no pitting in the lateral walls, which are continuous (homogenized) with the thickenings. Unfortunately, further splitting of the specimen failed to provide more information on the nature, number or distribution of these cells.

Comments: further specimens are clearly needed, but such limited evidence suggests similarities with the tracheids described in *Cooksonia pertoni* from the same locality (Edwards *et al*. 1992) and with those recovered from a sterile, coalified axis from the Upper Silurian (Whitcliffian) of South Wales. The latter are the earliest demonstrated in an axial fossil (Edwards & Davies 1976). Edwards (1999) suggested that this simple organization, viz non-perforate, relatively thick-walled cylinder plus further internal annular thickenings was the primitive type, and that secondary wall pitting between thickenings evolved in response to the pressures associated with major extension growth and increased requirements for lateral movement of water.

(c) *Anomalous conducting cells*

These were all recovered from central parts of axes, are elongate and longitudinally aligned, but vary in wall characters and in associations of the various types. The use of the term 'secondary thickening' for wall layering is avoided as there is, as yet, no information on development and the term has tracheophyte connotations. In many cases, the lateral walls of the elongate elements are undoubtedly layered and may show extensions, rods that line or project into the lumen, or sometimes folds. They are called lumen projections here.

(i) *Internally smooth-walled types*

(a) *Uniform thickening*

In these examples, the surface lining the lumen is smooth. Walls of adjacent cells are homogenized and are not very thick. Such cells are sometimes located at the centre of a strand comprising diverse types (see figure 8*c*), but in one example (figure 6*g*,*h*) are the only components of a discrete central strand. The surface of the short length of naked axis is smooth with broad, low ridges marking the elongate, uniformly thickened epidermal cells. Stomata are rare. The walls of the conducting cells are approximately the same as those of the epidermis. Viewed in SEM at low angles, there are some indications of transverse undulations. The cells are polygonal in fractured transverse section. Longitudinal fracture confirmed that their wide range in diameter results from tapering. There is no evidence for any developmental pattern.

Comments: elongate cells with smooth, pitted or non-perforate lateral walls characterize moss hydroids in general, although the thinner facets, generally quoted as forming by hydrolysis, but now interpreted as resulting from post-mortem cell extension, i.e. without chemical breakdown (Ligrone *et al*., this issue), are not represented as thinner walls in the fossils (Hébant 1974).

Elongate cells with uniformly thickened walls also occur in the central regions of axes of Rhynie Chert taxa, *Aglaophyton* (Edwards, D. S. 1986), while in *Nothia* (El-Saadawy & Lacey 1979) the preserved water-conducting cells are described as 'narrow with no detectable thickening or pitting', although the walls are more intensely coloured than in the rest of the tissues apart from the epidermis.

(b) *Lumen projections*

Here the surface lining the lumen is again smooth (i.e. not pitted or perforate) but bears various kinds of projections.

Dendritic. The unbranched single specimen has a smooth surface with longitudinal ridges, but is unusual in that the epidermis, although preserved, is inconspicuous because cortical cells are also preserved, and there is no well-defined central strand (figure 6*e*). The latter contains at least two cells with numerous irregular lumen projections that are much branched and completely lack any order (figure 6*f*). They may stand free or be adpressed to the cell wall, and are so numerous that the latter are difficult to see, but do not appear to contain pits.

Comments: these bizarre cells have no counterparts in extant or coeval plants. Fungal contamination remains a possibility.

Fretwork. In these examples the projections may be robust or fine, show limited branching and fusion, and may traverse the lumen (figure 8*f*) as well as looking like tracheidal annular to pitted secondary thickenings (figure 8*h*). The latter are continuous (homogenized) with the lateral walls. These examples, some of which show great complexity (e.g. figure 8*k*), come from a central strand of diverse composition (figure 8*c*) in contrast with similar cells, but with less regular thickenings in figure 6*d* where all the cells are the same. Figure 8*l*,*m* shows a central strand limited by a thick homogeneous rind, where all the cells, although of varying diameter, are characterized by fine ± branched projections.

Comments: comparisons with transfer cells may be appropriate here, although 'large-scale' pitting is absent in lateral walls in these examples.

Micropitted. These fall into two broad categories, both with or without projections, that may be flexuous or straight, depending on whether or not the perforate layer readily separates from the common homogenized wall between elements. Figure 8*g* shows an example of a separated layer *ca*. 300 nm thick that is extended into a ?hollow, rod-shaped projection. The perforations, *ca*. 40–90 nm diameter, may be simple or surrounded by a narrow rim (figure 8*i*). The latter example also shows occasional small globular outgrowths similar to forms that dominate the lumen surface of adjacent elements (figure 8*j*). It has not yet been possible to determine whether or not the perforations are in identical positions in adjacent cells (i.e. comparable with pit pairs) but this seems unlikely. The common homogenized wall is usually far less prominent than that illustrated in figure 8*g*. In no

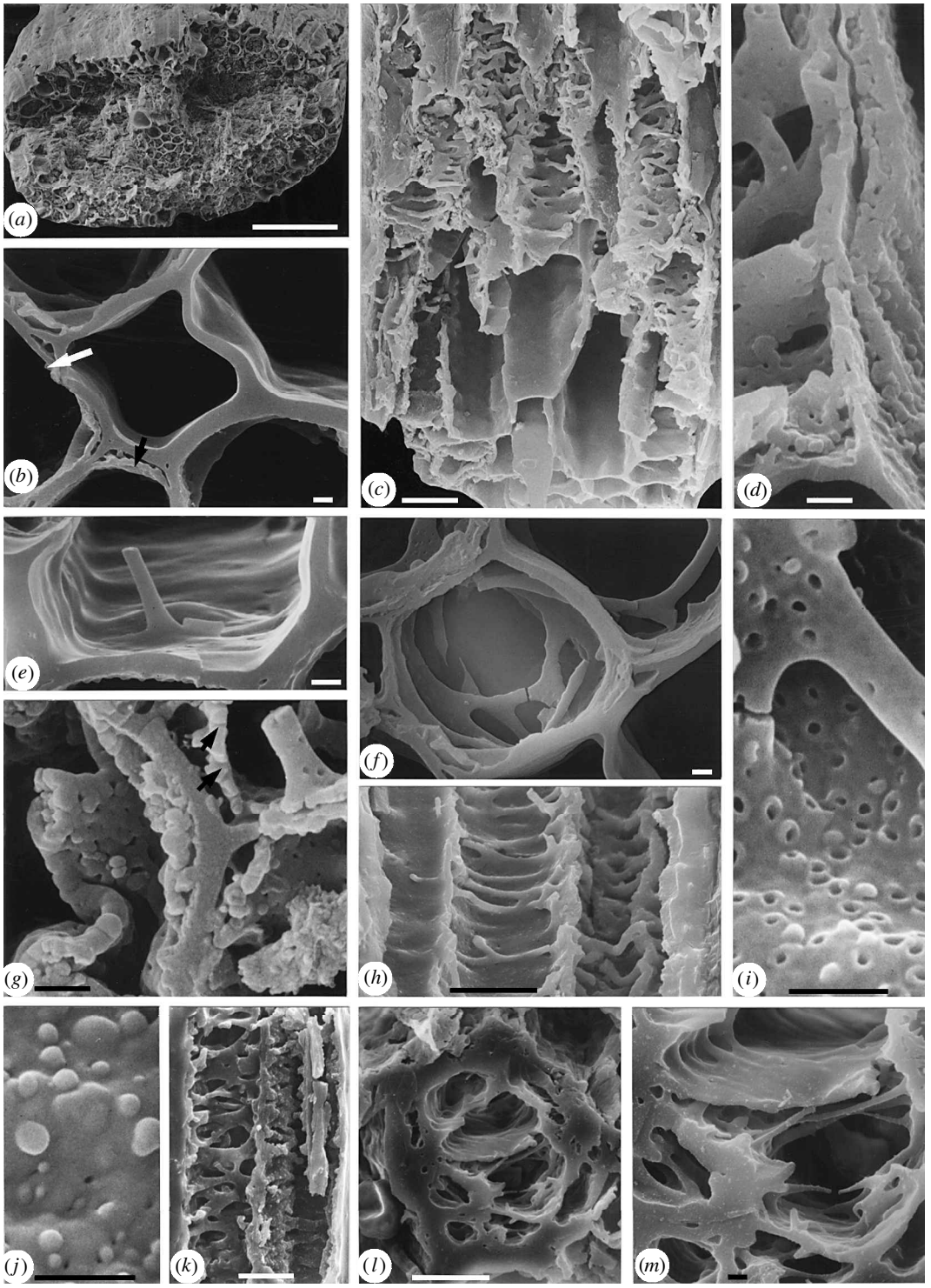

Figure 8. SEMs of presumed conducting cells. North Brown Clee Hill, Shropshire. Lochkovian, Lower Devonian. (*a–k*) Unbranched smooth coalified axis. NMW96.30G.1. (*a*) Transverse fracture showing stereome and central strand with well-preserved cells. Scale bar = 100 μm. (*b*) Evenly thickened smooth-walled cells to centre of central strand. Arrows indicate two adjacent cells with additional layer with smooth surface. Scale bar = 1 μm. (*c*) Oblique longitudinal fracture showing smooth central cells surrounded by those with internal thickenings. Scale bar = 10 μm. (*d*) Junction between two longitudinally fractured cells. To the left, the microperforate lining layer also occurs on projections into the lumen. To the right, cells with small granular projections on layer lining lumen. Scale bar = 1 μm. (*e*) Rare smooth projection into lumen in cell with otherwise uniformly thickened walls. Scale bar = 1 μm. (*f*) TS cell with complex smooth projections forming a fretwork. Scale bar = 1 μm. (*g*) Chaotic appearance in transversely fractured cells produced when microperforate layer becomes detached. Note that pits penetrate the latter (arrows). Scale bar = 1 μm. (*h*) Transversely orientated superficial thickenings in central cell. Scale bar = 10 μm. (*i*) Microperforate layer magnified to show rimmed pits and some globules. Scale bar = 1 μm. (*j*) Predominantly globules on surface. Scale bar = 1 μm. (*k*) Complex thickenings to margin of strand. Scale bar = 10 μm. (*l,m*) SEMs: smooth axis with small discrete central strand. NMW99.20G.9. (*l*) TS complete strand limited by irregular homogeneous layer. Scale bar = 10 μm. (*m*) Close up of cells with fine smooth strands traversing lumen. Scale bar = 1 μm.

example are adjacent walls completely perforate such that adjacent lumens are in continuity. In rare, as yet not fully investigated examples, the projections are convoluted, but sparingly branched and may occupy a considerable volume of the lumen (figure 8*e*,*f*). In others they are adpressed to the lumen wall, appearing similar to secondary thickenings (figure 6*k*). They occur in short lengths of unbranched axes and also in a unique example bearing short, apically incomplete enations (figure 7*g*,*i*), where stomata are also present (figure 7*h*). In the second type of wall thickening, there is no separation of a perforate layer and the pores are not parallel-sided but expand, such that in section they appear as minute bordered pits, although pit pairs are not present (figure 7*a*). The contours of exposed surfaces reflect the shape of the underlying cavities (figure 7*d*). In addition there are individual globules and groups of smooth ± spherical structures that may extend into the lumen as chains (figures 6*i* and 7*b*). Adjacent to elements of this type are those lacking well-defined pores, but where the internal surface bears a reticulum with bevilled edges (figure 7*c*). It is tempting to conclude that this is an immature wall.

(iii) *General comments on functions of cells from comparative anatomy*

Combinations of the various types of presumed conducting elements described above suggest that diversity in structure might be related to differences in function. The most instructive in this respect was the strand described by Edwards *et al*. (1998) in an axial, apparently astomatiferous, specimen lacking branching but with a prominent stereome. Additional illustrations are presented here (figure 8*a–k*). The central strand comprised at least four cell types, although these may intergrade (figure 8*b*). Its centre is occupied by tubular elements with essentially smooth (figure 8*c*), but sometimes gently transversely undulating walls (figure 8*e*), which in section have a completely uniform, featureless appearance, because adjacent walls are homogenized (figure 8*b*). Figure 8*e* shows a unique smooth projection. The surrounding cells again have imperforate walls, but these are extended into smooth rods, sometimes branched or anastomosing and traversing the lumen (figure 8*f*), or lie adjacent and are continuous with the lateral walls. In this respect they are similar to secondary thickenings (figure 8*h*). The most complex arrangement is shown in figure 8*k*. Elements with detaching microperforate layers occur to the outside of the strand, where projections are extensive, and sometimes appear quite disorganized (figure 8*c*,*g*). Inferences on the functions of the elements are hampered by lack of information on the chemistry of the walls. In coalified compression fossils of tracheophytes, preservation of conducting elements is related to the presence of the recalcitrant polymer lignin. Phloem is not preserved in such fossils. However, the presence of a wider range of cell types in these mesofossils leads to the possibility that predominantly cellulose cell walls are preserved. This may depend on wall thickness (e.g. in a stereome) or even presence of non-lignin polyphenols (e.g. see discussion on chemistry of the stereome in *Psilophyton dawsonii*, Edwards *et al*. 1997). In any event, inferences on the functions of the cells should not be constrained by preconceptions based on tracheophyte anatomy.

The featureless, smooth, relatively thin-walled cells whose length exceeds 200 μm, seen in the centre of the specimen and entirely composing the central strand, are closest to hydroids of mosses. The latter, as in the fossils, are usually strongly tapering with no pitting or perforations. They are almost invariably surrounded by leptoids. The thinner walls (facets) in moss hydroids (e.g. Hébant 1974) have not been seen in the fossils, although longitudinally fractured walls of the strand entirely composed of these elements show periodic lens-shaped thickenings corresponding to the undulations noted above. Such walls adjacent to the lumina also bear irregular films, possibly the residues of cell contents. Uniform wall width characterizes the central cells of *Aglaophyton major*, where an inner core of elongate thin-walled cells lacking intercellular spaces is surrounded by a cylinder of similar tissue but with thicker walls. In a re-evaluation of the central strand of *Aglaophyton*, D. S. Edwards (1986) concluded that (i) the innermost cells were comparable with polytrichaceous hydroids; (ii) they were surrounded by stereids with a presumed structural role; and (iii) the outermost tissue had similarities with moss leptoids. However, it should be emphasized that such an arrangement has no extact counterpart in extant bryophytes (Edwards 1993). The strand of smooth, thin-walled cells described here is closer in wall dimensions to those surrounding the central zone of putative hydroids. The spheres frequently recorded in the two central tissues and also in transfusion cells of *Aglaophyton* (Remy & Hass 1996) and regarded by some as silica artefacts (see discussion in Edwards, D. S. 1986; Edwards 1993), have not been seen in these smooth-walled, coalified fossils although spherical structures are present in cells with lumen projections. The cells with smooth internal projections are not so readily compared favourably with modern analogues. A structural role for the projections in water-conducting cells is a possibility, but they are far less regular than tracheidal secondary thickenings.

(iv) *Comparisons of micropitted cells*

A microporate layer lining the lumen characterizes S-type tracheids (Kenrick *et al*. 1991*a*), now considered diagnostic of the Rhyniopsida, including *Rhynia gwynne-vaughanii* and *Stockmansella* spp. (Kenrick & Crane 1991; Kenrick *et al*. 1991*b*). In the original descriptions based on demineralized pyrite permineralizations of *Sennicaulis hippocrepiformis*, the coalified underlying material occupying the position of the primary wall and helical 'secondary' thickenings was described as spongy (Kenrick *et al*. 1991*a*). It was suggested that the decay resistance of the microporate layer might be due to impregnation with an 'aromatic non-polysaccharide component' (possibly lignin). A similar explanation would be appropriate for the coalified residues in the spongy layer, but whether the spaces were filled with air, fluid or degradable polysaccharides such as cellulose or hemicelluloes remains conjectural. The pores did not extend through this layer, nor was a middle lamella detected. Comparing such organization with the coalified fossils here, the microporate layer of the S-type tracheid would be comparable with the inner porate layer and the spongy zone with homogenized adjacent walls, which could have been of less uniform composition in the living plant but homogenized on diagenesis. The pores in

the microporate layer of the S-type tracheid (majority *ca.* 100 nm diameter, range 40–200 nm) were believed to be plasmodesmata-derived, were longer and were much more evenly and densely spaced (16 μm^{-2}). The microporate layer in the S-type was thinner (100 nm versus *ca.* 300 nm). In both types, there is no evidence of perforation between adjacent cells. To date, no globular material has been recorded in the S-type tracheids, while the coalified fossils lack any regular helical thickenings.

Pitted and possibly perforate walls characterize the hydroids of gametophytes of metzgerialean liverworts (Hébant 1977; Frey *et al.* 1996). The *Symphyogyna* type has been described as most tracheid-like, in that the elongate, very narrow hydroids have walls of uneven thickness. Frey *et al.* (1996) and Ligrone & Duckett (1996) have recently confirmed that the thick wall is cellulose, primary and non-layered, with pits situated at the bases of oblique, slit-shaped depressions, *ca.* 0.3 μm diameter, and produced around plasmodesmata. Perforated examples are probably artefacts of preparation. They are thus totally unlike any tracheids or the cells described here. In contrast, the SEMs of internal surfaces of predominantly the end walls (not lateral walls) of *Haplomitrium* and *Takakia* look similar to some of the micropitted forms (Hébant 1979; Burr *et al.* 1974; Ligrone *et al.*, this issue). The cells themselves are slightly more elongate than the surrounding parenchymatous cells, and the non-layered walls are only slightly thicker (cf. the highly elongate, thick-walled cells in *Symphyogyna*). Hébant (1973) considered the *Haplomitrium* pits as truly perforate and arising from enlarged plasmodesmata. Such perforated 'pit pairs' have not been seen in the fossils. In *Takakia*, pores also occur in pairs and are derived from plasmodesmata, but are much smaller (Ligrone *et al.*, this issue). The specimen described here (figure 8*a–k*), with central strand composed of cells comparing favourably with moss-like hydroids surrounded by cells with lumen projections, some of which are micropitted, raises the possibility that the latter, since not obviously structural, were involved with food conduction. However, the organization of moss leptoids is far simpler, with thickened but undifferentiated lateral walls and the presence of many, sometimes enlarged, plasmodesmata in the end walls. There are no perforated end walls comparable with those in angiosperm sieve plates (Hébant 1977; Scheirer 1980), but the inclined end walls do resemble the simple sieve areas of sieve cells in certain ferns (Stevenson 1974). Recently discovered hepatic, food-conducting cells in both complex (Ligrone & Duckett 1994: *Asterella*) and simple (Ligrone *et al.*, this issue) thalloid liverworts have the same cytological organization as leptoids, with extensively thickened walls and highly structured plasmodesmata. The latter are sometimes associated with depressions and hence are comparable with primary pit fields, but there are no indications of perforations in living cells (Ligrone *et al.*, this issue).

Perhaps the most striking similarities of the cells with complex internal projections are with embryophyte transfer cells (Pate & Gunning 1972; Gunning 1977). Although from TEMs the architecture of the cell wall ingrowths is difficult to comprehend, SEM preparations involving an enzyme-etching method reveal a complex, three-dimensional branching and anastomous structure, possibly even more complex than those described here but in the same size range (e.g. Briarty 1974, where fig. 9-2 shows transfer cells adjacent to the xylem in a legume root nodule). Such preparations also show primary pit fields of irregular shape (restricted to the cell wall proper), quite unlike the small, circular pits in the fossil that occur on an additional inner layer of the wall as well as on the projections. In that transfer cells are widespread today at the junctions between gametophytes and sporophytes in bryophytes and 'pteridophytes' (Pate & Gunning 1972; Ligrone *et al.* 1993) and occur between gametophytic cortical cells and zygote in *Coleochaete* (Graham & Wilcox 1983), it is most likely that they existed in early embryophytes and that elongate cells of similar labyrinthian construction were involved, not in water transport, but as part of a food-conducting tissue system. However, the preservation of cells with such delicate extensions of the cellulose cell wall in coalified fossils stretches credulity even in a locality with fossils showing such exceptional preservation. Nevertheless, these new fossils do exhibit strands of diverse cells, for the most part not readily nor exactly matched by those in extant conducting cells. More information is now needed on the nature of the axes, e.g. whether or not branching or stomatiferous, on the chemical composition of cell walls and, most importantly, on fertile parts, be they gametophytic or sporophytic.

4. RECOGNITION OF EARLY BRYOPHYTES: A CASE HISTORY

The following account of a solitary, very fragmentary specimen demonstrates the kinds of problems encountered in trying to provide unequivocal evidence for early bryophytes in the fossil record.

(a) *Description* (*figures 9 and 10*)

The coalified axial fragment, *ca.* 600 μm long and 130 μm wide, has a saucer-shaped expansion at one end that is presumed to be the distal (figure 9*a–d*). The axial part shows gross striation and irregular, longitudinal ridging, suggestive of some shrinkage. Its surface also has some transverse ribbing, but microscopically is generally smooth except for occasional, small, crater-like bodies that are more prominent on the terminal expansion (figure 9*g*). At the proximal fractured surface, the axis is limited by a superficial homogeneous layer, *ca.* 3.0 μm thick, extended into longitudinal ridges (figure 9*e*), although near the margins, there are structures suggestive of thick-walled epidermal cells, whose inner walls are thinner than the outer. Unfortunately, this area is disorganized and it is impossible to detect any further cell layers, although irregular voids may be evidence for this (figure 9*e*). There are no indications of a distinct cuticle. The central area is occupied by a number of compressed, smooth-walled bodies with rounded topography and some adhering granules (figure 9*e*). These are spore tetrads. The axis widens to 330 μm distally. The surface ridging is not present on the expanded bevelled margin, although the presumed cuticle itself is continuous over the rim (figure 10*a–c*), where it becomes irregularly fragmented. Where it has broken away, a reticulum of shallow, isodiametric cells is seen below (asterisk in

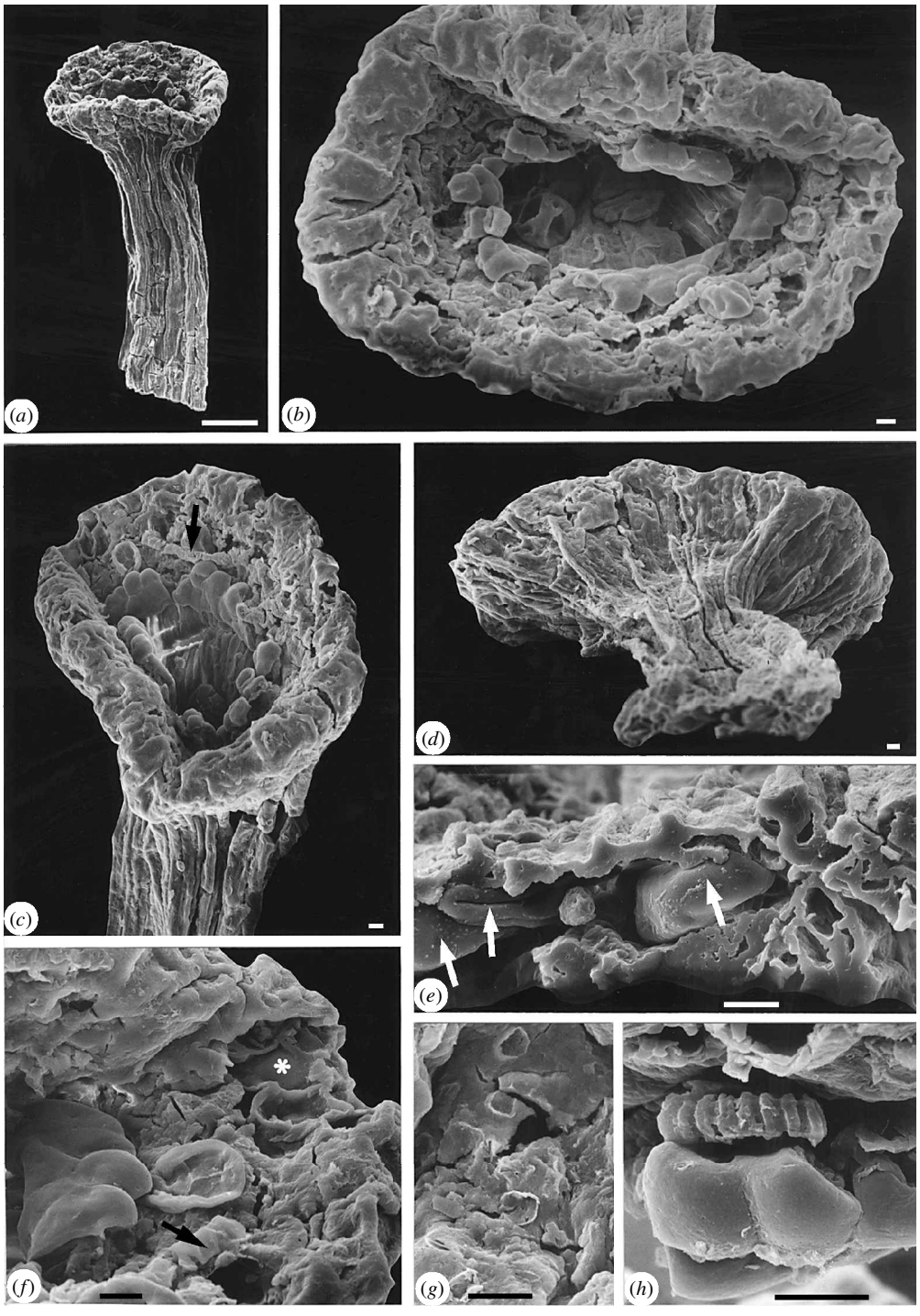

Figure 9. SEMs: unnamed specimen. North Brown Clee Hill, Shropshire. Lochkovian, Lower Devonian. NMW99.20G.10. Scale bars = 10 μm except (*a*). (*a*) Intact specimen with terminal expansion. Scale bar = 100 μm. (*b*) Terminal expansion from above. Note tetrad within hollow central area with incomplete lobed collar. (*c*) Same viewed from side. Note collar and possible elater (arrow). (*d*) Terminal expansion from below demonstrating continuity of superficial layer (?cuticle). (*e*) Fractured base of specimen. Note superficial thick walls and tetrads (arrows). (*f*) Surface of terminal expansion. Note lobed collar to left, exotic spore, end of ?elater (arrow) and periclinal fracture through epidermis (asterisk). (*g*) Cuticle with 'craters'. (*h*) Cast of possible elater lodged between collar and surface of terminal expansion (top).

figure 9*f*). From above, the central area of the terminal expansion is seen as a hollow cylinder (now compressed) *ca.* 135 μm diameter and lined by an irregular, ridged wall lacking any evidence for distinct cells, although the fractured surface suggests it comprised a layer of thick-walled cells with small lumens (figure 10*e*). Its surface is microscopically smooth, except for adhering irregular particles. Distally, the central cavity is limited by a very smooth, ring-like structure that is marginally and centrifugally lobed with rounded contours (figures 9*b*,*c* and 10*a*–*d*). It has not been possible to demonstrate continuity between this 'collar' and the ridged interior of the cavity. Indeed, the lobed edge overlaps the centripetally sloping margin that becomes increasingly disorganized in

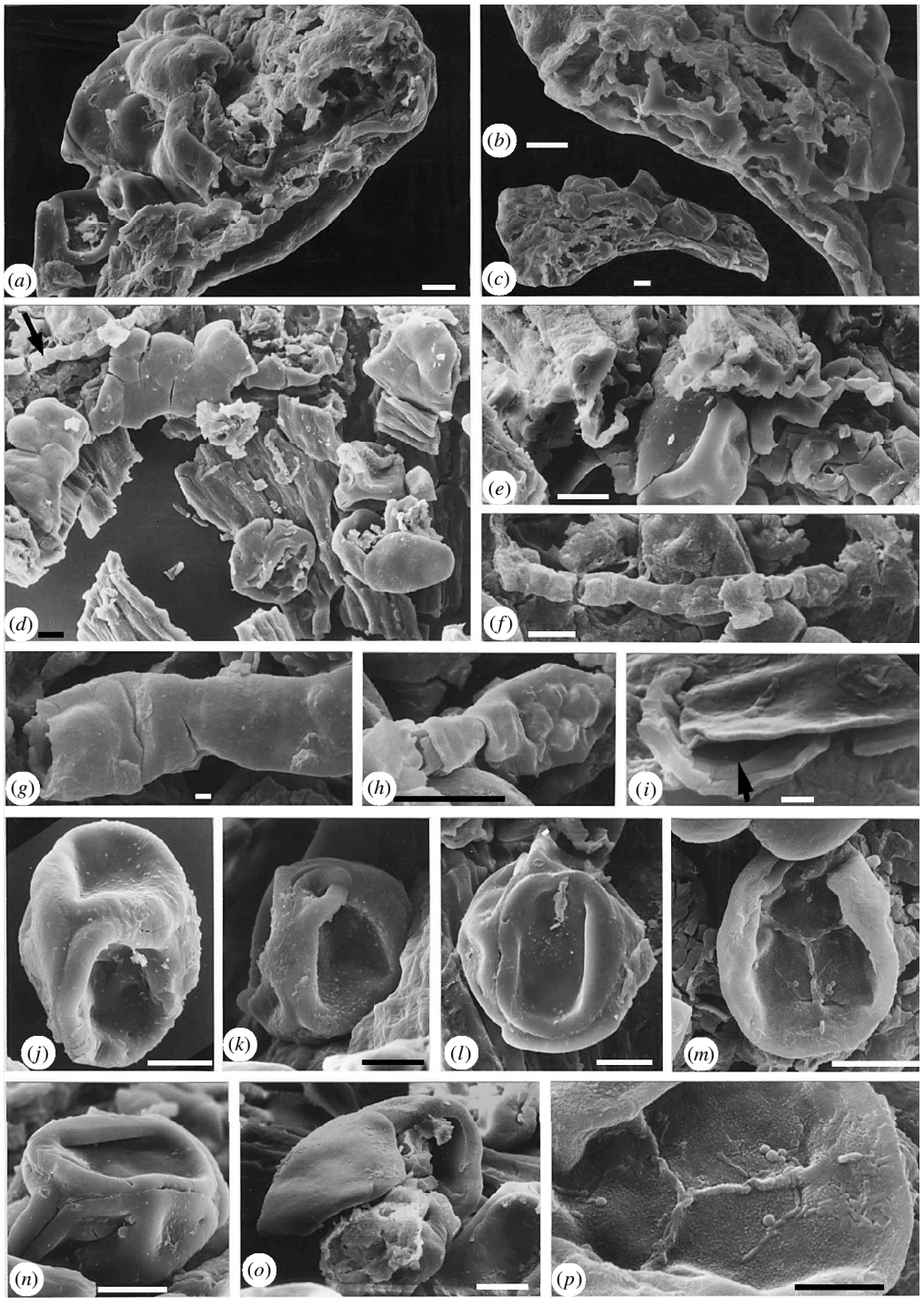

Figure 10. SEMs: unnamed specimen. North Brown Clee Hill, Shropshire. Lochkovian, Lower Devonian. NMW99.20G.10. Scale bars = 10 μm, except in (*g*), (*i*) and (*p*). (*a–c*) Longitudinally fractured terminal expansion showing relationship of collar to sporangial wall. (*d*) Fragmented inner surface of the 'axis' just below the collar. Note smooth longitudinal ridging and adhering tetrads. Arrow indicates possible elater. (*e*) Transverse fracture of hollow cylinder at base of terminal expansion showing lack of any cellular detail (outside at top) in cylinder surrounding the spores. (*f*) Possible elater. (*g,h*) Close-up of surface of elater in (*f*). (*g*) Scale bar = 1 μm. (*i*) Fractured elater. Internal thickening indicated by arrow. Scale bar = 1 μm. (*j–l,n*) Intact tetrads with predominantly smooth surface to ?envelope. Note some indications of separation particularly in (*l*) and (*n*). (*m*) Proximal surface of exotic monad with triradiate apertural fold adhering to the surface of the terminal expansion. (*o*) Partially separated tetrad with debris obliterating exposed proximal surfaces. (*p*) Part of (*m*) magnified showing microgranular surface and possible adhering bacteria. Scale bar = 5 μm.

this area. However, the isolated fragment illustrated in figure 10*a–c* shows that the superficial sloughing-off layer of the terminal expansion is continuous with the lower unexposed surface of the recurved flap, while its exposed surface is continuous with the thick walls forming the inner periclinal and anticlinal walls of the cells of the superficial layer (figure 10*a–c*). In contrast, the cells of the lower surface of the terminal expansion have thinner walls, but it is impossible to determine if there is more than one layer of cells in this region. The superficial cells

are more or less isodiametric in surface view on the edge, but become more elongate on the lower surface.

Adhering to the sides of the hollow cylinder are tetrads of spores (figure 10*d*,*e*). Occasional tetrads and a monad with triradiate apertural fold also occur on the rim (figure 9*b*,*f*), together with a short, cylindrical structure with broad, superficial grooves (figure 9*h*), and a longer but less 'complete' tubular structure with no obvious superficial details except for faint sporadic broad ridges (figure 10*f*–*h*). The former is interpreted as a cast of a structure with internal ridging. The tetrads (figure 10*j*–*n*) *ca.* 31 μm (28–35 μm; $n = 7$) in diameter are essentially smooth-walled, but with some adhering granules. Figure 10*k* shows an exceptional specimen where the granules are more or less evenly spaced. Using cryptospore terminology, they are fused in the sense that in the majority there is no line marking the junction between individual components, and the junction between three spores is marked by a depressed ± triangular area. However, all specimens show indications of splitting into separate components (e.g. figure 10*l*,*n*). The latter have a pronounced equatorial thickening accentuated by invaginated distal surfaces. One specimen shows evidence of more complete separation but, unfortunately, detritus obscures the original contact areas and any haptotypic features (figure 10*o*). The monad with distinct triradiate mark in figure 10*p* is unlikely to be related to the tetrads as it has a minute granular ornament on all surfaces. The figure also shows adhering putative bacteria, but whether these are recent or very ancient contaminants cannot be decided. I suspect the former.

(b) *Discussion*

The nature of terminal expansion is conjectural. Is it the sporangium? Or is it part of a complex terminal dehiscence structure of an elongate sporangium? The presumed hollow, ?cuticle-lined cylindrical structure is quite unlike anything else encountered in the Lochkovian assemblage, or indeed elsewhere. It is certainly not a conventional axis with central strand, and the presence of spores in the presumed proximal end suggests the whole structure was fertile. It is tempting to compare the ?cuticularized layer lining the cavity as homologous with the sporangial linings produced by the tapetum in a variety of Lower Devonian plants, e.g. *Resilitheca* (Edwards *et al.* 1995) and *Psilophyton* (Banks *et al.* 1975). Such an interpretation (viz elongate sporangium with distal dehiscence) finds no counterpart in extant embryophytes. However, elongate sporangia characterize the Anthocerotales, where the central part of the sporangium is occupied by a columella that produces the pseudoelaters. Since this region has already decomposed in the mature sporangium, it is broadly similar to the fossil. A major difference relates to dehiscence. In anthocerotes, the wall splits into two valves. In the fossil, the recurved lobed collar is an extension of the surface of the terminal expansion, which probably initially formed the roof of the sporangial cavity but then split centrifugally and curved outwards, producing a large central pore for spore escape. Distal poral dehiscence is rare in early land plants, being recorded only in a bifurcating cylindrical sporangium containing *Emphanisporites* cf. *micrornatus* from the Welsh Borderland locality and in *Horneophyton* (Edwards & Richardson (2000) and discussion therein). In both cases, the spores are monads with triradiate marks. The spores described here are in tetrads and in some cases resemble permanent tetrads, with no sutures between individual monads. In this state, they would be assigned to the dispersed taxon *Cheilotetras*. Most have laevigate distal surfaces—the irregular, adhering particles may demonstrate microbial activity or may be extra-exosporal residues. They are not considered a part of wall ornament. However, as is the case with the *in situ* tetrads illustrated in figures 2 and 3, some show indications of separation, with remarkably 'clean' fracture lines. Frustratingly, in the one showing most separation (figure 10*o*), haptotypic features are obscured by debris. It is tempting to relate these tetrads to examples thought to demonstrate hepatic affinities in Ordovician and Silurian early land plants, or possibly to consider them as being produced by relict populations of the plants that first evolved separation of tetrads for dispersal in the Late Ordovician/Early Silurian (Steemans *et al.* 1996). Associated with the spores are two structures, one tubular and one a cast, that may be elaters. The cast of a tubular lumen has spiral or annular depressions that are broad and deep, presumably reflecting internal thickenings of a tubular structure (figure 9*h*). Similarities to tracheids and the 'banded' tubes initially assigned to nematophytes (Lang 1937) are obvious, but in the latter, the thickenings are narrower and more closely spaced. The longer, flattened tubular structure shows only faint indications of internal thickenings of diverse widths (figure 10*h*), interpretation being hampered by external adhering fragments and internal growth of pyrite. Their identification as elaters is based on their position and gross similarities with extant forms, demonstrated as possessing recalcitrant polymers and hence with enhanced fossilization potential (Kroken *et al.* 1996). Their position may also be considered evidence for their being residues of a bryophyte sporangial wall, although the length of the tubular one does not support this. That they are pathogenic, as proposed for tubes with much smaller and closely spaced thickenings mentioned elsewhere in this paper (p. 5), is discounted on their size and their isolation from any form of the debris that characterizes microbial films. However, cratering of the cuticle associated with decay is present on the surface of the expanded region.

Thus, although in this small specimen hepatic characters may be present, its overall organization finds no counterpart in extant liverworts. Its proposed dehiscence mechanism is unique. On the other hand, it cannot be demonstrated to be a tracheophyte either.

5. RECOGNITION OF BRYOPHYTE SPOROPHYTES IN THE FOSSIL RECORD

(a) *Unbranched sporophytes*

The unequivocal demonstration of absence of branching in a fragmentary fertile sporophyte presents insuperable problems. The majority of fertile specimens recovered from this Lochkovian locality comprise terminal sporangia borne singly on short lengths of unbranched axes. In longer specimens, branching is sometimes preserved. What is needed is a large number of specimens of varying length, all of which have

unbranched axes. This was the case for *Sporogonites exuberans*, where large obovate- to club-shaped sporangia terminate unbranched axes at least 12 cm long. Some rock surfaces show parallel alignment of these axes, and although the irregular coalified film that Andrews (1960) thought represented a thalloid gametophyte merely overlies the bases of the axes, *S. exuberans* remains the most compelling earliest fossil bryophyte candidate. The axes in *Sporogonites* are very straight and of uniform width, such that they give the impression of great rigidity as is found in the setae of mosses. Stomata at the base of the sporangium and a possible, but equivocal columella (Halle 1916, 1936; Edwards *et al*. 1998) reinforce moss affinity, although Halle (1916) concluded that it was a sporangium of the Bryophyta of a 'generalized' type.

Consistent absence of branching accompanied by axial twisting prompted (Edwards 1979) to postulate bryophyte (possibly hepatic) affinity for Upper Silurian *Tortilicaulis transwalliensis*. Subsequent demonstration of twisting in Silurian sterile branching axes at another locality and the discovery of Lower Devonian specimens (Edwards *et al*. 1994) with similarly shaped sporangia with trilete spores and twisting in both axes and sporangia, weakens bryophyte affinity for the older specimens, but anatomical evidence in the latter is essential to establish that the same genus is involved.

(b) *Sporangial characters*

These were reviewed at length by Edwards *et al*. (1998). My comments here are thus not comprehensive.

Spore configurations provide evidence for the existence of plants at a bryophyte grade in the Ordovician/Silurian (Gray 1985) and their ultrastructure points to sphaerocarpalean affinity (Taylor 1997). The value of similar forms when preserved in sporangia remains more controversial, particularly where the producers have branching sporophytes. The demonstration of elaters in sporangia would strengthen the existence of hepatics. To date, there are two possible *in situ* records, but much larger numbers of elaters per sporangium are required to allow more detailed analysis. Kroken *et al*.'s (1996) suggestion that some of the banded tubes in the dispersed record might be elaters deserves further attention.

There is a considerable amount of information on the construction of the sporangium wall, including possible tapetal layers and dehiscence mechanisms, in early tracheophytes and rhyniophytoids where spores are almost all trilete. A few examples have sporangial stomata, a character shared with certain mosses, but they are rarely concentrated near the base of the sporangium (Edwards *et al*. 1996). I doubt it would be possible to distinguish a bryophyte using only sporangial wall characters, particularly in the absence of complex dehiscence mechanisms found in mosses. The recent suggestions that differentially thickened walls of cells from certain moss and liverwort sporangia that survive acetolysis are similar to the banded (i.e. differentially thickened) tubes found in Silurian and Devonian sediments (Kroken *et al*. 1996) demands further testing. To date, all the examples recovered in our studies are long and radially symmetrical tubes, often associated with wefts of smaller tubes. In the mesofossils at this Lower Devonian locality, individual cells in the sporangial wall may be thickened, usually to different degrees in anticlinal and periclinal walls, but not spirally. Kroken *et al*. also suggested that some of the dispersed sheets with reticulate patterning reflecting underlying cellular organization, which are often considered cuticles of the *Nematothallus* complex, also derive from bryophyte sporangia. We have recently shown that the chemical composition of such cuticles differs from those of tracheophytes in that they are predominantly aromatic rather than aliphatic (Edwards *et al*. 1996). They thus have a different source from sporangial cuticles recorded, often with adhering trilete spores, but sometimes dyads (figure 4*a*) from Wenlock and younger sediments. As mentioned earlier, we need to know more about the precise chemistry of tissues in extant fossils and indeed in bryophytes, although whether such information will be of value in detecting affinities in view of the effects of diagenesis on complex aromatic molecules remains uncertain (see discussion in Ewbank *et al*. 1997).

(c) *Axial anatomical features*

The various kinds of conducting cells described here, although difficult to interpret in terms of function, demonstrate the potential of such fossils to preserve bryophyte tissues. Structures less likely to be preserved are rhizoids. These are preserved by silica in the Rhynie Chert and are unicellular (see review in Edwards 1993) in both tracheophytes (e.g. *Rhynia*, *Trichopherophyton*) and *Aglaophyton*, which is one of the few Rhynie Chert taxon reputed to have some bryophyte characters. The other is *Horneophyton*, which has columellate sporangia with complex poral dehiscence structures (e.g. Eggert 1974) terminating otherwise homoiohydric aerial axes. Indeed, the absence of unequivocal bryophytes in the Rhynie terrestrial ecosystems, which have been so intensively researched, is a major mystery, especially as bryophytes can be pioneering colonizers on highly stressed substrates in modern hot-spring analogues (e.g. New Zealand; Burns 1997).

6. CONCLUDING REMARKS

'We see what we know'—our searches for evidence for fossil bryophytes are constrained by data based on extant representatives. The fossil record of bryophytes is very poor compared with other plant groups, although occasional records (e.g. *Naiadita*) provide tantalizing combinations of characters not seen in extant form (Hemsley 1989). An alternative approach is prompted by Mishler & Churchill's (1985) reconstruction of a number of archetypes based on shared homologies. Thus, for example, the archetype of land plants was reconstructed as a thalloid gametophyte with single sessile sporangium and that for the moss-tracheophyte clade as a radially symmetrical, leafless, branched gametophyte with conducting tissues and stomata. A coalified fossil of the latter might appear as a collection of branching axes with a single terminal sporangium. Here, the single sporangium and perhaps the demonstration of a discontinuity of some sort at the sporophyte/gametophyte junction would provide good evidence for a fossil bryophyte in the absence of anatomy, but demands a new approach to the examination of existing material. The recent palaeobotanical research reported here indicates that the fossil

record is now producing new combinations of characters and novel character states, and makes the search for new and older fossiliferous horizons imperative. The Ordovician/Silurian dispersed spore record also demands further investigation of the kind initiated by Taylor (e.g. 1995*a*,*b*, 1997). It is quite remarkable that in a time interval that is hypothesized to have seen the emergence of liverworts and mosses, there is apparent stasis in terms of named taxa in composition of dispersed spore assemblages (Wellman 1996), apart from the appearance of monads. Superficial ornament shows little of the diversity recorded later in the Silurian and Devonian (probably explained by the presence of envelopes), but investigations of ultrastructure in the same species through time might reveal evidence of change.

REFERENCES

Andrews, H. N. 1960 Notes on Belgian specimens of *Sporogonites*. *The Palaeobotanist* **7**, 85–89.

Banks, H. P., Leclercq, S. & Hueber, F. M. 1975 Anatomy and morphology of *Psilophyton dawsonii*, sp.n. from the late Lower Devonian of Quebec (Gaspé), and Ontario, Canada. *Palaeontographica Americana* **8**, 77–127.

Bell, P. R. 1992 *Green plants. Their origin and diversity*. Cambridge University Press.

Bierhorst, D. W. 1960 Observations on tracheary elements. *Phytomorphology* **10**, 249–305.

Briarty, L. G. 1974 Plant cell walls and intracellular structures. In *Principles and techniques of scanning electron microscopy. Biological applications*, vol. 1 (ed. M. A. Hayat), pp. 206–225. New York: Van Nostrand Reinhold Company.

Brown, R. C. & Lemmon, B. E. 1990 Sporogenesis in bryophytes. In *Microspores: evolution and ontogeny* (ed. S. Blackmore & R. B. Knox), pp. 55–94. London: Academic Press.

Burgess, N. D. & Richardson, J. B. 1991 Silurian cryptospores and miospores from the type Wenlock area, Shropshire, England. *Palaeontology* **34**, 601–628.

Burns, B. 1977 Vegetation change along a geothermal stress gradient at the Te Kopia steamfield. *J. R. Soc. NZ* **27**, 279–294.

Burr, R. J., Butterfield, B. G. & Hébant, C. 1974 A correlated scanning and transmission electron microscope study of the water-conducting elements in the gametophytes of *Haplomitrium gibbsiae* and *Hymenophyton flabellatum*. *The Bryologist* **77**, 612–617.

Cook, M. E. & Friedman, W. E. 1998 Tracheid structure in a primitive extant plant provides an evolutionary link to earliest fossil tracheids. *Int. J. Plant Sci.* **159**, 881–890.

Crandall-Stotler, B. 1986 Morphogenesis, developmental anatomy and bryophyte phylogenetics: contraindications of monophyly. *J. Bryol.* **14**, 1–2.

Dunleavy, J. A. & McQuire, A. J. 1970 The effect of water-storage on the cell structure of sitka spruce (*Picea sitchensis*) with reference to its permeability and preservation. *J. Inst. Wood Sci.* **5**, 20–28.

Edwards, D. 1979 A late Silurian flora from the Lower Old Red Sandstone of south-west Dyfed. *Palaeontology* **22**, 23–52.

Edwards, D. 1993 Tansley Review No. 53. Cells and tissues in the vegetative sporophytes of early land plants. *New Phytol.* **125**, 225–247.

Edwards, D. 1996 New insights into early land ecosystems: a glimpse of a Lilliputian world. *Rev. Palaeobot. Palynol.* **90**, 159–174.

Edwards, D. 1998 Climate signals in Palaeozoic land plants. *Phil. Trans. R. Soc. Lond.* B **353**, 141–157.

Edwards, D. 1999 Origins of plant architecture: adapting to life in a brave new world. In *The evolution of plant architecture* (ed. M. H. Kurmann & A. R. Hemsley), pp. 3–21. Kew: Royal Botanic Gardens.

Edwards, D. & Davies, E. C. W. 1976 Oldest recorded *in situ* tracheids. *Nature* **263**, 494–495.

Edwards, D. & Richardson, J. B. 2000 Progress in reconstructing vegetation on the Old Red Sandstone Continent: two *Emphanisporites* producers from the Lochkovian of the Welsh Borderland. Geological Society of London Special Publication. (In the press.)

Edwards, D., Davies, K. L. & Axe, L. 1992 A vascular conducting strand in the early land plant *Cooksonia*. *Nature* **357**, 683–685.

Edwards, D., Fanning, U. & Richardson, J. B. 1994 Lower Devonian coalified sporangia from Shropshire: *Salopella* Edwards & Richardson and *Tortilicaulis* Edwards. *Bot. J. Linn. Soc.* **116**, 89–110.

Edwards, D., Fanning, U., Davies, K. L., Axe, L. & Richardson, J. B. 1995 Exceptional preservation in Lower Devonian coalified fossils from the Welsh Borderland: a new genus based on reniform sporangia lacking thickened borders. *Bot. J. Linn. Soc.* **117**, 233–254.

Edwards, D., Abbott, G. D. & Raven, J. A. 1996 Cuticles of early land plants: a palaeoecophysiological evaluation. In *Plant cuticles—an integrated functional approach* (ed. C. Kerstiens), pp. 1–31. Oxford: BIOS Scientific Publishers.

Edwards, D., Ewbank, G. & Abbott, G. D. 1997 Flash pyrolysis of the outer cortical tissues in Lower Devonian *Psilophyton dawsonii*. *Bot. J. Linn. Soc.* **124**, 345–360.

Edwards, D., Wellman, C. H. & Axe, L. 1998 The fossil record of early land plants and interrelationships between primitive embryophytes: too little too late? In *Bryology for the 21st century* (ed. J. W. Bates, N. W. Ashton & J. G. Duckett), pp. 15–43. British Bryological Society and Maney Publishing.

Edwards, D., Wellman, C. H. & Axe, L. P. 1999 Tetrads in sporangia and spore masses from the Upper Silurian and Lower Devonian of the Welsh Borderland. *Bot. J. Linn. Soc.* **130**, 111–156.

Edwards, D. S. 1986 *Aglaophyton major*, a non-vascular land plant from the Devonian Rhynie Chert. *Bot. J. Linn. Soc.* **93**, 173–204.

Eggert, D. A. 1974 The sporangium of *Horneophyton lignieri* (Rhyniophytina). *Am. J. Bot.* **61**, 405–413.

El-Soadawy, W. El-S. & Lacey, W. S. 1979 Observations on *Nothia aphylla* Lyon ex Høeg. *Rev. Palaeobot. Palynol.* **27**, 119–147.

Ewbank, G., Edwards, D. & Abbott, G. D. 1997 Chemical characterization of Lower Devonian vascular plants. *Org. Geochem.* **25**, 461–473.

Fanning, U., Richardson, J. B. & Edwards, D. 1988 Cryptic evolution in an early land plant. *Evol. Trends Plants* **2**, 13–24.

Fanning, U., Edwards, D. & Richardson, J. B. 1991 A new rhyniophytoid from the late Silurian of the Welsh Borderland. *Neues Jb. Geol. Paläontol. Abh.* **183**, 37–47.

Frey, W., Hilger, H. H. & Hofmann, M. 1996 Water-conducting cells of extant *Symphogyna*-type Metzgerialean taxa: ultrastructure and phylogenetic implications. *Nova Hedwigia* **63**, 471–481.

Graham, L. E. & Wilcox, L. W. 1983 The occurrence and phylogenetic significance of tentative placental transfer cells in the green alga *Coleochaete*. *Am. J. Bot.* **70**, 113–120.

Graustein, J. E. 1930 Evidence of hybridism in *Selaginella*. *Bot. Gaz.* **90**, 46–73.

Gray, J. 1985 The microfossil record of early land plants: advances in understanding of early terrestrialization, 1970–1984. *Phil. Trans. R. Soc. Lond.* B **309**, 167–195.

Gray, J. 1991 *Tetrahedraletes*, *Nodospora*, and the 'cross' tetrad: an accretion of myth. In *Pollen and spores, patterns of diversification* (ed.

S. Blackmore, & S. H. Barnes), pp. 49–87. The Systematics Association special vol. 44. Oxford: Clarendon Press.
Gray, J. & Boucot, A. J. 1971 Early Silurian spore tetrads from New York: earliest New World evidence for vascular plants? *Science* **173**, 918–921.
Gunning, B. E. S. 1977 Transfer cells and their roles in transport of solutes in plants. *Sci. Prog.* **64**, 539–568.
Halle, T. G. 1916 A fossil sporogonium from the Lower Devonian of Röragen in Norway. *Botaniska Notiser* 79–81.
Halle, T. G. 1936 Notes on the Devonian genus *Sporogonites*. *Svensk Bot. Tidskr.* **30**, 613–623.
Hébant, C. 1973 Diversity of structure of the water-conducting elements in liverworts and mosses. *J. Hattori Bot. Lab.* **37**, 229–234.
Hébant, C. 1974 Studies on the development of the conducting tissue-system in the gametophytes of some Polytrichales. II. Development and structure at maturity of the hydroids of the central strand. *J. Hattori Bot. Lab* **38**, 565–607.
Hébant, C. 1977 *The conducting tissues of bryophytes*. Bryophytorum Bibliotheca 10. Vaduz: J. Cramer.
Hébant, C. 1979 Conducting tissues in bryophyte systematics. In *Bryophyte systematics* (ed. G. C. S. Clarke & J. G. Duckett), pp. 365–383. The Systematics Association special vol. 14. London: Academic Press.
Hemsley, A. R. 1989 The ultrastructure of the spore wall of the Triassic bryophyte *Nadiadita lanceolata*. *Rev. Palaeobot. Palynol.* **61**, 89–99.
Hickok, L. G. & Klekowski, E. J. 1973 Abnormal reductional and nonreductional meiosis in *Ceratopteris*: alternatives to homozygosity and hybrid sterility in homosporous ferns. *Am. J. Bot.* **60**, 1010–1022.
Kenrick, P. & Crane, P. R. 1991 Water-conducting cells in early land plants: implications for the early evolution of tracheophytes. *Bot. Gaz.* **152**, 335–356.
Kenrick, P. & Edwards, D. 1988 The anatomy of Lower Devonian *Gosslingia breconensis* Heard based on pyritized axes, with some comments on the permineralization process. *Bot. J. Linn. Soc.* **97**, 95–123.
Kenrick, P., Edwards D. & Dales, R. C. 1991*a* Novel ultrastructure in water-conducting cells of the Lower Devonian plant *Sennicaulis hippocrepiformis*. *Palaeontology* **34**, 751–766.
Kenrick, P., Remy, W. & Crane, P. R. 1991*b* The structure of the water-conducting cells in the enigmatic early land plants *Stockmansella langii* Fairon-Demaret, *Huvenia kleui* Hass et Remy and *Sciadophyton* sp. Remy *et al*. 1980. *Argumenta Palaeobot.* **8**, 179–191.
Kroken, S. B., Graham, L. E. & Cook, M. E. 1996 Occurrence and evolutionary significance of resistant cell walls in charophytes and bryophytes. *Am. J. Bot.* **83**, 1241–1254.
Lang, W. H. 1937 On the plant-remains from the Downtonian of England and Wales. *Phil. Trans. R. Soc. Lond.* B **227**, 245–291.
Levy, J. F. 1975 Bacteria associated with wood in ground contact. In *Biological transformation of wood by micro-organisms* (ed. W. Liese), pp. 60–73. Berlin: Springer.
Ligrone, R. & Duckett, J. G. 1994 Thallus differentiation in the marchantialean liverwort *Asterella wilmsii* (Srepb.) with particular reference to longitudinal arrays of endoplasmic microtubules in the inner cells. *Ann. Bot.* **73**, 577–586.
Ligrone, R. & Duckett, J. G. 1996 Development of water-conducting cells in the antipodal liverwort *Symphyogyna brasiliensis* (Metzgeriales). *New Phytol.* **132**, 603–615.
Ligrone, R., Renzaglia, K. S. & Duckett, J. G. 1993 The gametophyte–sporophyte junction in land plants. *Adv. Bot. Res.* **19**, 231–317.
Lugardon, B. 1990 Pteridophyte sporogenesis: a survey of spore wall ontogeny and fine structure in a polyphyletic plant group. In *Microspores, evolution and ontogeny* (ed. S. Blackmore & R. B. Knox), pp. 95–120. London: Academic Press.
Mishler, B. D. & Churchill, S. P. 1984 A cladistic approach to the phylogeny of the 'bryophytes'. *Brittonia* **36**, 406–424.
Mishler, B. D. & Churchill, S. P. 1985 Transition to a land flora: phylogenetic relationships of the green algae and bryophytes. *Cladistics* **1**, 305–328.
Mishler, B. D., Lewis, L. A., Buchheim, M. A., Renzaglia, K. S., Garbary, D. J., Delwiche, C. F., Zechman, F. W., Kantz, T. S. & Chapman, R. L. 1994 Phylogenetic relationships of the 'green algae' and 'bryophytes'. *Ann. Mo. Bot. Gdn* **81**, 451–483.
Morzenti, V. M. 1967 *Asplenium plenum*: a fern which suggests an unusual method of species formation. *Am. J. Bot.* **54**, 1061–1068.
Pate, J. S. & Gunning, B. E. S. 1972 Transfer cells. *A. Rev. Plant Physiol.* **23**, 173–196.
Remy, W. & Hass, H. 1996 New information on gametophytes and sporophytes of *Aglaophyton major* and inferences about possible environmental adaptations. *Rev. Palaeobot. Palynol.* **90**, 175–193.
Richardson, J. B. 1988 Late Ordovician and Early Silurian cryptospores and miospores from northeast Libya. In *Subsurface palynostratigraphy of northeast Libya* (ed. A. El-Arnauti, B. Owens & B. Thusu), pp. 89–109. Benghazi, Libya: Garyounis University Publications.
Richardson, J. B. 1996 Taxonomy and classification of some new Early Devonian cryptospores from England. *Spec. Pap. Palaeontol* **55**, 7–40.
Scheirer, D. C. 1980 Differentiation of bryophyte conducting tissues: structure and histochemistry. *Bull. Torrey Bot. Club* **107**, 298–307.
Schuster, R. M. 1967 Studies on Hepatica, XV. Calobryales. *Nova Hedwigia* **12**, 3–64.
Steemans, P., Le Herisse, A. & Bozdogan, N. 1996 Ordovician and Silurian cryptospores and miospores from southeastern Turkey. *Rev. Palaeobot. Palynol.* **93**, 35–76.
Stevenson, D. W. 1974 Ultrastructure of the nacreous leptoids (sieve elements) in the polytrichaceous moss *Atrichum undulatum*. *Am. J. Bot.* **61**, 414–421.
Taylor, W. A. 1995*a* Spores in earliest land plants. *Nature* **373**, 391–392.
Taylor, W. A. 1995*b* Ultrastructure of *Tetrahedraletes medinensis* (Strother and Traverse) Wellman and Richardson, from the Upper Ordovician of southern Ohio. *Rev. Palaeobot. Palynol.* **85**, 183–187.
Taylor, W. A. 1996 Ultrastructure of lower Paleozoic dyads from southern Ohio. *Rev. Palaeobot. Palynol.* **92**, 269–279.
Taylor, W. A. 1997 Ultrastructure of lower Paleozoic dyads from southern Ohio II: *Dyadospora murusattenuata*, functional and evolutionary considerations. *Rev. Palaeobot. Palynol.* **97**, 1–8.
Wellman, C. H. 1996 Cryptospores from the type area of the Caradoc Series in southern Britain. *Spec. Pap. Palaeontol.* **55**, 103–136.
Wellman, C. H. & Richardson, J. B. 1993 Terrestrial plant microfossils from Silurian inliers of the Midland Valley of Scotland. *Palaeontology* **36**, 155–193.
Wellman, C. H., Edwards, D. & Axe, L. 1998 Ultrastructure of laevigate hilate cryptospores in sporangia and spore masses from the Upper Silurian and Lower Devonian of the Welsh Borderland. *Phil. Trans. R. Soc. Lond.* B **353**, 1983–2004.

Discussion

P. Kenrick (*Department of Palaeontology, The Natural History Museum, London, UK*). Sporophyte branching is completely absent in the normal course of development of modern liverworts, hornworts and mosses. The absence of apical growth during the ontogeny of these groups (except for very limited apical cell divisions in mosses) explains why this is the case and indicates that their sporophytes were

never branched. Furthermore, the lack of a sporophyte generation in the charophycean algal ancestors of land plants is consistent with the idea that the earliest land plants would have had very simple, unbranched sporophytes. How does one reconcile these data with fossil evidence indicating that sporophytic branching is plesiomorphic for embryophytes as a whole?

D. Edwards. Dr Kenrick refers to the very limited evidence presented in my paper for sporophytic branching in plants containing dyads and tetrads. These fossils come from Lower Devonian rocks; we have no megafossil evidence for the polyad producers before this. They may well have lacked sporophytic branching. The presence of polyads in the Lower Devonian plants may just indicate the retention of a stem-group bryophytic character. Evidence for the nature of conducting cells in these fossils would help to resolve this issue.

The possibility of loss of sporophytic branching in bryophytes deserves further consideration and is one that might be appropriately addressed in a functional genomics programme.